Effects of Different Interfacial Modifiers on the Properties of Digital Printing Waste Paper Fiber/Nano-Crystalline Cellulose/Poly (Lactic Acid) Composites*

xiaolin zhang (zxlbmm@sina.com)
xi'an university of technology
Jingjing Di
Xi'an University of Technology
Jia Li
Xi'an University of Technology
Shaoge Li
Xi'an University of Technology
Jingting Duan
Xi'an University of Technology
Jinyan Lv
Xi'an University of Technology
Yi Wang
Xi'an University of Technology
Xiaofeng Zhu
Xi'an University of Technology
Long Xu
Xi'an University of Technology

Research Article

Keywords: digital printing waste paper fiber, nano-crystalline cellulose, poly (lactic acid), interfacial modifier, composites, diffusion coefficient

Posted Date: June 8th, 2021

DOI: https://doi.org/10.21203/rs.3.rs-556876/v1

Effects of different interfacial modifiers on the properties of digital printing waste paper fiber/nano-crystalline cellulose/poly (lactic acid) composites*

Xiaolin Zhang*, Jingjing Di, Jia Li, Shaoge Li, Jingting Duan, Jinyan Lv, Yi Wang, Xiaofeng Zhu, Long Xu

(*Faculty of Printing, Packaging Engineering and Digital Media, Xi'an University of Technology, Xi'an, Shaanxi Province, China,* 710048)

Abstract： Digital printing waste paper fiber/nano-crystalline cellulose/poly (lactic acid) (DPF/NCC/PLA) composites, modified through γ-methacryloxy propyl trimethoxy silane (KH570), isopropyl tri (dioctylpyrophosphate) titanate (TMC201), sodium hydroxide (NaOH), polyethylene glycol 6000 (PEG6000), and a composite silane coupling agent (KH570/PEG6000), were fabricated by melt blending and injection molding and the effects of different modifiers on the properties of composites were studied. Results showed that mechanical properties of the modified composites generally improved, and the best mechanical properties, including flexural, tensile and impact strength, were achieved PEG6000, KH570/PEG6000, and KH570 modification, respectively. Thermal performance analysis showed improved thermal properties of composites treated by KH570, but the crystallinity of the modified materials was increased. Both water absorption and degradation properties showed a decreasing trend, and water absorption performance was obviously improved after KH570/PEG6000 modification. Under the action of several modifiers, the diffusion coefficient, thermodynamic solubility and permeability of composites were reduced to varying degrees. Furthermore, scanning electron microscopy (SEM) demonstrated that interfacial adhesion and composite compatibility were improved with significantly fewer and smaller pores, as well as a fuzzy boundary among the three phases.

Keywords: digital printing waste paper fiber; nano-crystalline cellulose; poly (lactic acid); interfacial modifier;

Correspondence

Xiaolin Zhang, Faculty of Printing, Packing Engineering and Digital Media Technology, Xi'an University of Technology, Xi'an 710048, Shaanxi, China.

Email: zxlbmm@sina.com

composites; diffusion coefficient

1 Introduction

With the continuous development of an industrial society, non-renewable resources such as petroleum resources and plastic products have been consumed in enormous quantities, and their non-degradability has brought severe environmental problems. In recent years, the public's awareness of environmental protection has gradually strengthened, and research on composite materials technology has made progress. Therefore, environmentally friendly composite materials have attracted the attention of researchers worldwide.

Poly (lactic acid) (PLA), derived from renewable resources, such as starch, is an ideal biodegradable polymer material[1], which can be completely decomposed to obtain carbon dioxide and water under specific conditions, such as composting and combustion, to realize an ecological carbon cycle originated from nature and attributed to nature. PLA has preferable mechanical strength and excellent biocompatibility, degradation, and sustainable utilization[2], but at the same time, it is limited by its chemical structure, resulting in poor toughness, poor hydrophilicity, slow crystallization rate and great brittleness, thus limiting widespread applications. Nano-crystalline cellulose (NCC) is a new type of biodegradable and renewable nanomaterial, which has good thermal stability, high strength, high crystallinity and other properties, and can improve wide variety of composite materials. Existing studies have shown that NCC can strengthen the characteristic defects of PLA materials[3-6]. Similarly, strengthening resin with plant fiber can also effectively improve its performance defects[7-10].

In the printing industry, digitally printed papers are becoming a larger proportion of the incoming waste paper stream to the recycling industry and increasing amounts of digital prints from offices accounts for a certain proportion of the recovered paper[11]. For traditional recycling methods, waste paper is mostly used as raw material for recycled paper. However, deinking of digital prints involves a deeper understanding of the ink and its interactions with various types of substrates[12]. Consequently, even though digital printing waste paper has excellent fiber quality, it is rarely used in the production of recycled paper and provides little added value. Therefore, the efficient utilization of digital printing waste paper attracts much attention. Blending filled digital printing waste paper fiber (DPF) can reduce the production cost of composite materials, and the utilization of DPF is economical and environment-friendly, has ample sources, and easily obtained, which can realize the idea of “turning waste into

treasure"[13]. Therefore, in this paper, we will study the performance of a ternary DPF/NCC/PLA degradable composite material with DPF as the blend filler material, PLA as the matrix and NCC as the reinforcement, which is not only of academic significance, but also of great practical importance.

In this study, DPF was used as the blending filler material to prepare NCC/PLA composites, and the modifier was used to react with PLA and cellulose to improve the interfacial conditions and the composite properties[14-17]. Modifiers, such as γ-methacryloxy propyl trimethoxy silane (KH570), isopropyl tri (dioctylpyrophosphate) titanate (TMC201), sodium hydroxide (NaOH), polyethylene glycol 6000 (PEG6000) and composite silane coupling agent (KH570/PEG6000), were added to the composite material. DPF/NCC/PLA composites were prepared by melt blending and injection molding process, and the influence of different modifiers on DPF/NCC/PLA composite material was studied. The structural properties of the prepared degradable composites were analyzed and characterized by mechanical properties, Fourier transform infrared spectroscopy (FTIR), thermogravimetry (TG), differential scanning calorimetry (DSC), and scanning electron microscopy (SEM).

2 Materials and methods

2.1 Materials

DPF was obtained from the local digital printing waste paper of Xi'an, Shaanxi, China. NCC was prepared from DPF using a sodium hydroxide (NaOH) treatment and sulfuric acid (H_2SO_4) solution with a mass fraction of 66% in our laboratory. PLA (3052D) was purchased from Nature Works (America). KH570 (Nanjing Chuangshi Chemical Co. Ltd., Nanjing, China), TMC201 (Dongguan Dinghai Plastic Chemical Co. Ltd., Dongguan, China), NaOH (Zhengzhou Paini Chemical Reagent Factory, Zhengzhou, China), PEG6000 (Tianjin Damao Chemical Reagent Factory, Tianjin, China) and KH570/PEG6000 were used as interfacial modifiers for WP/NCC/PLA composite materials respectively. Ethanol and phosphate buffered saline (PBS) were provided by Tianjin Fuyu Fine Chemical Co. Ltd (Tianjin, China) and Xiamen Haibiao Technology Co. Ltd (Xiamen, China), respectively.

2.2 Composite fabrication

According to the mass ratio of 90:10, anhydrous ethanol aqueous solution was prepared and utilized as the solvent, and 3%KH570, 3%TMC201, 5%NaOH, 4%PEG6000 and KH570/PEG6000, respectively, were used as the solute and then sprayed onto 3% NCC and 15% DPF. The solvent was

evaporated by drying in an oven at 80 °C for 12 h after reacting in a water bath at 60 °C for 5 h. DPF, NCC, and PLA were blended and melted by the twin rotary mixer XH-401C (Dongguan, China) at 170 °C, and five composite samples were prepared by the injection molding machine TA-150 (Ningbo, China) at 170 °C and 9 MPa injection pressure. Besides that, the overall processing techniques of NCC and DPF/NCC/PLA modified composite preparations are schematically shown in Figure 1.

3 Testing and characterization

3.1 Mechanical property testing

The mechanical properties of standard samples of modified DPF/NCC/PLA composites were tested by universal testing machine XWW-20A (Shanghai, China) and impact testing machine YF-8109 (Yangzhou, China). The flexural and tensile performances of the samples were tested according to GB/T 1449-2005 and GB/T 1447-2005 standards with loading speeds of 2 mm/min and 10 mm/min, respectively. Then, the impact performance test was carried out in accordance with the GB/T 1043-1993 standard at a loading gear of 25 J and an impact angle of -150°.

3.2 Fourier transform infrared spectroscopy testing

Using a tablet press, the NCC and DPF modified samples were separately cold pressed with potassium bromide (KBr) powder to prepare test samples, which were then scanned and analyzed by the 8400S Fourier transform infrared spectrometer (FTIR) (SHIMADZU, Japan), including the test band range of 500~4000 cm^{-1} with 32 scanning times and a resolution of 4.0.

3.3 Thermogravimetric testing

The thermogravimetric (TG) curves of the modified composites were drawn using a STA 449F3 thermogravimetric analyzer (NETZSCH, Germany) over a temperature range of 30 to 600°C in an argon (Ar) atmosphere with a 40 mL/min flow rate, and at a constant heating rate of 20°C/min.

3.4 Differential scanning calorimetry testing

Differential scanning calorimetry (DSC) was performed on a DSC 200F3 thermal analysis instrument (NETZSCH, Germany) with two cycles (with a 5 min interval between them) at 200℃ to eliminate trace of thermal history[18]. The first cycle was carried out from 20℃ to 200℃ under a nitrogen flow of 60 mL/min followed by cooling from 200℃ to 20℃. Then, a second heating was performed from 20℃ to 200℃. All heating scans were performed at a rate of 10℃/min. The composite crystallinity (χ) was calculated using following equation (1)[19]:

$$\chi = \frac{\Delta H_m}{\Phi \Delta H_m^0} \times 100 \quad (1)$$

where ΔH_m, Φ and ΔH_m^0 are the melting enthalpy of the composite, mass fraction of PLA in the composite, and the theoretical enthalpy of fully crystallized PLA, which is 93.7 J/g[17,20], respectively

3.5 Water absorption testing

The water absorption of the modified DPF/NCC/PLA composites were investigated in accordance with GB/T 1034-2008. At room temperature, the samples were immersed in water for seven consecutive weeks. The water absorption percentage (MA) of the composite was calculated using following the equation (2):

$$MA = \frac{M_{TA} - M_{0A}}{M_{0A}} \times 100 \quad (2)$$

where M_{TA} and M_{0A} are the weight after and before water absorption, respectively.

The diffusion coefficient (D) was calculated based on the initial slope of the water absorption curve:

$$D = \pi \left(\frac{h}{4M_b}\right)^2 \left(\frac{M_2 - M_1}{\sqrt{t_2} - \sqrt{t_1}}\right)^2 \quad (3)$$

where, h is the specimen thickness, M_b is the balanced water absorption, M_2 and M_1 are the water absorption at t_2 and t_1, respectively.

Furthermore, the thermodynamic solubility (S) can be calculated by the following formula:

$$S = \frac{m_b}{m_c} \quad (4)$$

where m_b and m_c are the mass of absorbed water at equilibrium and composite materials mass, respectively.

Permeability was obtained by the product of diffusion coefficient and solubility:

$$P = D \times S \quad (5)$$

3.6 Degradation performance testing

To simulate the soil degradation environment, the samples were placed in phosphate buffer saline (PBS) (pH=7.8) at room temperature for continuous soaking over 90 days. The degradation rate (MD) of the composite was calculated using the following equation (3):

$$MD = \frac{M_{0D} - M_{TD}}{M_{0D}} \times 100 \quad (6)$$

where M_{0D} is the quality before degradation, and M_{TD} is the quality after degradation.

3.7 Scanning electron microscopy testing

Scanning electron microscopy (SEM) of the tensile fracture surfaces of the composites were

performed with a SU-8000 scanning electron microscope (HITACHI, Japan). Prior to testing, the samples were coated with a thin layer of conductive material (gold), and then observed under a scanning voltage of 10 kV and a magnification of 1000 times.

4 Results and discussion

3.1 Mechanical property analysis

Figure 2 presents the flexural properties of modified DPF/NCC/PLA composites. It can be seen that the flexural strength and modulus of the composites were improved to some extent with the addition of interfacial modifier. After modification with KH570, TMC201, NaOH, PEG6000, and KH570/PEG6000, the flexural strengths reached 98.3, 95.8, 100.4, 101.2 and 99.1 MPa, respectively, among which PEG6000 showed the highest improvement with a 6% increase in flexural strength. The flexural modulus increased by 7%, 13%, 2%, 12%, 1%, respectively, which means that the rigidity of the PLA matrix has increased with the addition of modifier[21].

The tensile strength and elongation at break of the modified DPF/NCC/PLA composites given in Figure 3 show that the tensile strengths of the composites modified with KH570, NaOH, PEG6000 and KH570/PEG6000 improved to 65.6, 65.1, 66.8 and 68.6 MPa, respectively, but a decrease is observed with the addition of TMC201. For elongation at break, the addition of NaOH shows no changes before and after modification, and KH570, TMC201, PEG 6000, KH570/PEG6000 increased by 12%, 7%, 5%, 12% respectively. Therefore, with the addition of modifiers, the toughness of the composites has been improved.

Figure 4 illustrates the impact properties of modified DPF/NCC/PLA composites. After adding KH570, TMC201, NaOH, PEG6000, and KH570/PEG6000, the impact strengths increased by 19%, 3%, 5%, 12%, and 15%, respectively. This shows that when KH570 is added, the impact properties are most improved with impact strengths reaching 12 KJ/m^2, which is then followed by the addition of KH570/PEG6000.

In general, the mechanical properties of the modified composites have been improved to varying degrees. The flexural strength, tensile strength, and impact strength show the most significant improvements with the additions of PEG6000, KH570/PEG6000, and KH570, and show improvements of 6%, 8%, and 19% respectively, when compared with the values prior to modification. The reason is that the -Si-OH produced after the hydrolysis of KH570 is dehydrated to bond with the

polar hydroxyl (-OH) on the surface of DPF and NCC, which can then be grafted with PLA through hydrogen bonding to make the interfacial bonding of the composites more compact[22], as shown in Figure 5 (a). At the same time, the surface of the reinforced materials becomes more wrinkled after modification, and a strong mechanical interlocking with the molecular chain of PLA is generated, so that DPF, NCC and PLA matrix have better compatibility and stronger adhesion. PEG6000 with multiple hydroxyl-terminated groups not only increases the contact between the enhancer and matrix through chemical bonding with the hydroxyl groups on the surface of DPF and NCC[23], but also conducts an esterification reaction, which is compatible with PLA and able to increase toughness[24-25]. The composite silane coupling agent, KH570/PEG6000, provides a synergistic effect of the above two.

3.2 Fourier transform infrared spectroscopy analysis

The molecular structure of cellulose provides a basis for its surface modification due to the multitude of hydroxyl groups[26]. The FTIR spectra of NCC and DPF after interfacial modification are shown in Figures 6 and 7, respectively. Near 3370 cm^{-1} is the stretching vibration peak of -OH, which decreases after modification, and is caused by the reduction of -OH groups after reacting with the modifier. The FTIR spectra also shows peaks at 1720 and 1634 cm^{-1}, which correspond to the characteristic absorptions of C=O and C=C after modification with KH570[27], further indicating that KH570 was been successfully grafted. However, TMC201 is chemically and directly coupled by its alkoxy group to the hydroxyl group on the cellulose surface, but no corresponding characteristic groups are generated in the coupling reaction, and the connection is still the -O-Ti bond, as shown in Figure 5 (b). Therefore, the grafting effect can only be judged by the -OH and $-CH_3$ groups on the cellulose surface. Thus, in addition to the weakened stretching vibration peak of -OH at 3370 cm^{-1}, the slight stretching vibration peak of $-CH_3$ and $-CH_2$ at 2961 cm^{-1} also indicate that TMC201 has been successfully grafted to the cellulose surface[28].

3.3 Thermogravimetric analysis

Thermogravimetric analysis of modified DPF/NCC/PLA composites are presented in Figures 8 and 9, and all of the corresponding data are given in Table 1. The TG curves of the modified composites show that the onset decomposition temperatures of the composites modified by TMC201, NaOH, PEG6000, and KH570/PEG6000 are reduced to different degrees compared with that before modification, as well as the temperature of maximum decomposition rate, indicating that these

modifiers have adverse effects on the thermal stability of the composites, especially the NaOH treatment. The maximum decomposition temperatures of the composites modified by KH570 are increased because the long chain alkanes of KH570 were successfully introduced onto the surface of DPF and NCC, and a coating layer was formed. The thermal stabilities of the composites were improved by absorbing some energy to destroy the interaction force and then pyrolyzing itself. The onset temperature of the composites modified by KH570 remains unchanged, while the maximum decomposition temperature increases, which is due to the fact that the KH570 long-chain alkanes were introduced onto the surface of DPF and NCC successfully, forming a coating layer and providing better cross-linking. In the thermal decomposition process, it is necessary to absorb a certain amount of energy to destroy the force between the two, and then pyrolysis takes place, so the thermal stability of the modified composites is improved[29]. Meanwhile, Table 1 shows that the residual amount of the modified composites increases, which is likely related to the residual organic modifier added to the composite material.

3.4 Differential scanning calorimetry analysis

Figure 10 presents heat flow endo up vs. temperature of the modified DPF/NCC/PLA composites. Table 2 shows the thermal parameters of DSC. The secondary heating curves show that the glass transition temperature (T_g) of the modified composites slightly decreased, while the T_g of the KH570 modified composites have a slight increase. After modification, the crystallization temperature (T_c) of composites is offset to the left, i.e. the T_c decreased, especially with the addition PEG6000, which shows a decreased from 122.9 to 109.3°C after modification, indicating that the modifiers can promote the movement of the PLA chain segment[30], and provide the ability to block the crystallization process of the composites. This may be attributed to more restricted molecular movements of PLA chains due to the formation of hydrogen bonds[31]. As the DSC heating curves demonstrate, bimodal endothermic melting peaks could be seen for all samples except the material modified with KH570. Among which, the lower one corresponds to crystalline melting with low perfection and thinner lamella and the higher peak is related to the melting of more perfect recrystallized crystals[32]. It can be seen from Table 2 that the crystallinity of the modified composites is improved, because the addition of modifier promotes the movement of the PLA molecular chain segment, which enables the molecular chain in the crystal region of the composite to regularly arrange[17].

3.5 Water absorption analysis

The cellulose molecules contain hydroxyl groups that attract water molecules through hydrogen bonding, causing the fiber to expand and absorb water[33-35]. Interfacial bonding between fiber and resin is also an important factor affecting the water absorption properties of composites. Figure 11 illustrates the effect of modifier on the water absorption behavior of DPF/NCC/PLA composites. It shows that water absorption increases with increasing immersion time for all modified samples. The water uptake rate is linear and very rapid in the beginning of the exposure, but then slows and reaches a saturation level. In the initial stage, the unmodified DPF/NCC/PLA showed a faster rate of water absorption, which was due to the hydrophilic properties of cellulose fibers, and the abundant hydroxyl groups that attract water molecules through hydrogen bonds, which in turn lead to fiber swelling and water absorption. At the same time, the fiber has a hollow cavity in the center, allowing a large amount of water to be absorbed by the capillary effect[36]. In addition, the small amount of water absorption of the PLA matrix and the gap water absorption existing in the combination of PLA, NCC and DPF are also important reasons for the high water absorption rate. After modification, the water absorption of the composites decreased to some extent. Among them, KH570/PEG6000 decreased the most, followed by PEG6000, NaOH, KH570, and TMC201, and the reduction reached 23%, 21%, 20%, 19% and 18% after seven weeks, respectively. This can be attributed to the reaction of modifiers with -OH on the cellulose surface, which reduced the amount of -OH, resulting in decreased of polarity and hydrophilicity. Furthermore, the interfacial affinity between reinforcement and matrix was improved with a more compact internal structure which reduced the water absorption rate of the gap after modification, so that the water absorption rate of the composites was improved. Due to the synergistic effect of the two modifiers, the water absorption properties of the composite modified by KH570/PEG6000 significantly improved.

The parameters related to water absorption of composites, including diffusion coefficient, thermodynamic solubility and permeability, are shown in Table 3. The water absorption behavior of composite materials (water diffusion behavior in composite materials) is usually represented by diffusion mechanism, which basically conforms to Fick water absorption model[37]. Compared with the unmodified DPF/NCC/PLA, the diffusion coefficients of the composites with the addition of the modifiers decreased, that is, the diffusion velocity of water molecules in the micro-gaps between the

polymer chains decreased[38]. It may be that the interface binding between cellulose molecular chains and matrix was improved under the action of modifiers. Through the reaction between the modifiers and the hydroxyl group on the surface of the cellulose, the hydrophilicity of the cellulose molecular chains was weakened, resulting in the decrease of the gap between the cellulose molecular chains and the hydrophobic PLA molecular chains, and therefore the diffusion coefficient reduced. In addition, the parameters of thermodynamic solubility and permeability can also help to further clarify the kinetic behavior of water absorption. The solubility is related to the absorption of the penetrant to a certain extent[37]. With the addition of the modifiers, the diffusion channel of water was inhibited, and the penetrant was prevented from penetrating the DPF/NCC/PLA composites, resulting in the decrease of solubility and permeability values.

3.6 Degradation performance analysis

Due to acid degradation, unstable chemical bonds (such as ester bonds) in PLA molecules freely hydrolyze and lead to chain scission, resulting in reduced relative molecular weight of PLA[7]. After degradation in PBS solution for 90 days, the DPF/NCC/PLA composite suffered from corrosion with the surface roughened and cracked, which resulted in destruction of the basic structure and composite morphology. The degradation performance of the modified DPF/NCC/PLA composites immersed in PBS for 90 days is shown in Figure 12. With increased water absorption, the degradation rate of the DPF/NCC/PLA composites reduced, especially with the addition KH570/PEG6000, which was then followed by PEG6000, NaOH, KH570, and TMC201, showing decreases from 5% to 3%, 3%, 4%, 4% and 4%, respectively. The lower degradation rate obtained for modified DPF/NCC/PLA composites is attributed to the modifier introduction which increases interfacial compactness, affects the contact area with phosphoric acid and, consequently, lowers the acid degradation rate[39].

3.7 Scanning electron microscopy analysis

SEM images of the samples, with different modifiers added during the preparation process of composites, are reported in Figure 13. After modification, a change in the section morphology of the composites is observed. A clear surface defect with fibers exposed and several tiny holes on the surface of the DPF/NCC/PLA composites are observed in Figure 12a, which shows that the bonding with the matrix is not tight enough, and the adhesion and interfacial compatibility between the two are poor. Figures 12b, c, d, e, and f demonstrate that DPF in the modified composite is firmly embedded in the

PLA matrix with significantly fewer and smaller pores as well as a fuzzy boundary between the fibers and the matrix, which leads to improved interfacial adhesion and composite compatibility. Therefore, the mechanical properties of DPF/NCC/PLA composites after modification have comprehensively improved.

5 Conclusion

In this paper, DPF/NCC/PLA composites modified with different modifiers were prepared by melt blending and injection molding. The mechanical, thermal, water absorption, and degradation properties of the composites, as well as micro-morphology, were investigated. FTIR analysis showed that the modifiers had been successfully applied to the composites. With the addition of modifiers, the interfacial bonding force between reinforced phase fiber and PLA was improved, so that the mechanical properties of the composites were further enhanced. Thermal property analysis showed that the thermal properties of KH570 were slightly improved after modification, while all others had adverse effects on the composites, but their crystallinity was improved. After modification, both water absorption and degradation properties were reduced, and the water absorption performance was improved most obviously after KH570/PEG6000 treatment, which was attributed to the improved interfacial bonding of the modified composites. Furthermore, SEM demonstrated that interfacial adhesion and composite compatibility were improved with significantly fewer and smaller pores as well as fuzzy boundary among the three phases.

Acknowledgments

The authors gratefully acknowledge financial supports from the key scientific research project of Education Department of Shaanxi Province (20JY051) and the key project of Science and Technology Department of Shaanxi Province(2021SF-448).

ORCID

Xiaolin Zhang https://orcid.org/0000-0002-1232-9781

References

[1] Liu GM, Zhang XQ, Wang DJ (2014) Tailoring crystallization: Towards high-performance poly (lactic acid). Adv Mater 26: 6905-6911. https://doi.org/10.1002/adma.201305413

[2] Boubekeur B, Belhaneche-Bensemra N, Massardier V (2015) Valorization of waste jute fibers in developing

low-density polyethylene/poly lactic acid bio-based composites. J Reinf Plast Comp 34: 649-661. https://doi.org/10.1177/0731684415576354

[3] Dasana YK, Bhata AH, Faizb A (2017) Polymer blend of PLA/PHBV based bionanocomposites reinforced with nanocrystalline cellulose for potential application as packaging material. Carbohyd Polym 157: 1323-1332. https://doi.org/10.1016/j.carbpol.2016.11.012

[4] Xu CJ, Lv QL, Wu DF, Wang ZF (2017) Polylactide/cellulose nanocrystal composites: a comparative study on cold and melt crystallization. Cellulose 24: 2163-2175. https://doi.org/10.1007/s10570-017-1233-x

[5] Aydemir D, Gardner DJ (2020) Biopolymer blends of polyhydroxybutyrate and polylactic acid reinforced with cellulose nanofibrils. Carbohyd Polym 250. https://doi.org/10.1016/j.carbpol.2020.116867

[6] Patel DK, Dutta SD, Hexiu J, Ganguly K, Lim KT (2020) Bioactive electrospun nanocomposite scaffolds of poly(lactic acid)/cellulose nanocrystals for bone tissue engineering. Int J Biol Macromol 162: 1429-1441. https://doi.org/10.1016/j.ijbiomac.2020.07.246.

[7] Xu C, Zhang XL, Jin X, Nie SJ, Yang RN (2019) Study on mechanical and thermal properties of poly (lactic acid)/poly (butylene adipate-co-terephthalate)/office wastepaper fiber biodegradable composites. J Polym Environ 27: 1273-1284. https://doi.org/10.1007/s10924-019-01428-9

[8] Behalek L, Boruvka M, Brdlik P, Habr J, Lenfeld P, Kroisova D, Veselka F, Novak J (2020) Thermal properties and non-isothermal crystallization kinetics of biocomposites based on poly (lactic acid), rice husks and cellulose fibres. J Therm Anal Calorim 142: 629-649. https://doi.org/10.1007/s10973-020-09894-3

[9] Bayart M, Adjalle K, Diop A, Ovlaque P, Barnabe S, Robert M, Elkoun S (2020) PLA/flax fiber bio-composites: effect of polyphenol-based surface treatment on interfacial adhesion and durability. Compos Interface. https://doi.org/10.1080/09276440.2020.1773179

[10] Arias A, Heuzey MC, Huneault MA (2013) Thermomechanical and crystallization behavior of polylactide-based flax fiber biocomposites. Cellulose 20: 439-452. https://doi.org/10.1007/s10570-012-9836-8

[11] Voss D, Putz HJ, Schabel S (2012) Deinking of recovered paper mixtures containing digital prints-challenges and prospects. Nip28: 28th International Conference on Digital Printing Technologies/Digital Fabrication 522-525

[12] Bhattacharyya MK, Ng HT, Mittelstadt LS, Aronhime M, Effects of paper on LEP digital print deinking with alkaline and neutral chemistries. Nip28: 28th International Conference on Digital Printing Technologies /Digital Fabrication 526-529

[13] Das S, Basak S, Bhowmick M, Chattopadhyay SK, Ambare MG (2016) Waste paper as a cheap source of natural

fibre to reinforce polyester resin in production of bio-composites. J Polym Eng 36: 441-447. https://doi.org/10.1515/polyeng-2015-0263

[14] Jin KY, Tang YJ, Zhu XM, Zhou YM (2020) Polylactic acid based biocomposite films reinforced with silanized nanocrystalline cellulose. Int J Biol Macromol 162: 1109-1117. https://doi.org/10.1016/j.ijbiomac.2020.06.201

[15] Fortunati E, Peltzer M, Armentano I, Torre L, Jiménez A, Kenny JM (2012) Effects of modified cellulose nanocrystals on the barrier and migration properties of PLA nano-biocomposites. Carbohyd Polym 90: 948-956. https://doi.org/10.1016/j.carbpol.2012.06.025

[16] Chen TT, Wu YC, Qiu JH, Fei MG, Qiu RH, Liu WD (2020) Interfacial compatibilization via in-situ polymerization of epoxidized soybean oil for bamboo fibers reinforced poly (lactic acid) biocomposites. Compos Part A Appl S 138. https://doi.org/10.1016/j.compositesa.2020.106066

[17] Zhang XL, Li SG, Xu C, Li J, Wang Z (2020) Study on the mechanical and thermal properties of poly (lactic acid)/office waste paper fiber composites. J Appl Polym Sci 137. https://doi.org/10.1002/app.49390

[18] Quitadamo A, Massardier V, Iovine V, Belhadj A, Bayard R, Valente M (2019) Effect of cellulosic waste derived filler on the biodegradation and thermal properties of HDPE and PLA composites. Processes 7. https://doi.org/10.3390/pr7100647

[19] Osman H, Ismail H, Mariatti M (2010) Comparison of reinforcing efficiency between recycled newspaper (RNP)/carbon black (CB) and recycled newspaper (RNP)/silica hybrid filled polypropylene (PP)/natural rubber (NR) composites. J Reinf Plast Compos 29: 60-75. https://doi.org/10.1177/0731684408096414

[20] Yeh JT, Tsou CH, Huang CY, Chen KN, Wu CS, Chai WL (2010) Compatible and crystallization properties of poly(lactic acid)/poly(butylene adipate-co-terephthalate) blends. J Appl Polym Sci 116: 680-687. https://doi.org/10.1002/app.30907

[21] Alamri H, Low IM (2012) Microstructural, mechanical and thermal characteristics of recycled cellulose fiber-halloysite epoxy hybrid nanocomposites. Polym Compos 33: 589-600. https://doi.org/10.1002/pc.22163

[22] Wu GH, Liu SQ, Wu XY, Ding XM (2016) Influence of MWCNTs modified by silane coupling agent KH570 on the properties and structure of MWCNTs/PLA composite film. J Polym Res 23. https://doi.org/ 10.1007/s10965-016-1024-3

[23] Qu P, Zhou YT, Zhang XL, Yao SY, Zhang LP (2012) Surface modification of cellulose nanofibrils for poly (1actic acid) composite application. J Appl Polym Sci 125: 3084-3091. https://doi.org/10.1002/app.36360

[24] Park BS, Song JC, Park DH, Yoon KB (2012) PLA/chain-extended PEG blends with improved ductility. J Appl Polym Sci 123: 2360-2367. https://doi.org/10.1002/app.34823

[25] Mohapatra AK, Mohanty S, Nayak SK (2016) Properties and characterization of biodegradable poly (lactic acid) (PLA)/poly (ethylene glycol) (PEG) and PLA/PEG/organoclay: A study of crystallization kinetics, rheology, and compostability. J Thermoplast Compos Mater 29: 443-463. https://doi.org/10.1177/0892705713518812

[26] Zhu HL, Luo W, Ciesielski PN, Fang ZQ, Zhu JY, Henriksson G, Himmel ME, Hu LB (2016) Wood-derived materials for green electronics, biological devices, and energy applications. Chem Rev 116: 9305-9374. https://doi.org/10.1021/acs.chemrev.6b00225

[27] An WF, Hu YM, Zhang DD, Li MM (2020) Optimization and characterization of surface modification of tourmaline by silane coupling agent KH570. Multipurpose Utilization of Mineral Resources.

[28] Xie CZ, Wang R, Zeng LL, Xu HS, Zhang FZ (2020) Effect of modified nano ZnO on thermal properties of room temperature vulcanized silicone rubber. High Volt Eng 46: 1337-1345. https://doi.org/10.13336/j.1003-6520.hve.20200430025

[29] Du XL, Xiong YM, Jin JB, Song JL, Long XB (2020) Study on surface modification of plant fiber and mechanical properties of PP composites. Chin Plast Ind 48: 114-117. https://doi.org/10.3969/j.issn.1005-5770.2020.08.025

[30] Bai SY, Han CY, Ni ZJ, Ni YH, Lv Y, Ye XP (2020) Effect of polyethylene glycol (PEG) on properties of the surface modified cellulose nanofiber (CNF)/polylactic acid (PLA) composite. J Forestry Eng 5: 62-68. https://doi.org/10.13360/j.issn.2096-1359.201906031

[31] Malmir S, Montero B, Rico M, Barral L, Bouza (2017) Morphology, thermal and barrier properties of biodegradable films of poly (3-hydro-xybutyrate-co-3-hydroxyvalerate) containing cellulose nanocrystals. Compos Part A Appl S 93: 41-48. https://doi.org/10.1016/j.compositesa.2016.11.011

[32] Lin N, Jin H, Chang PR, Feng J, Yu J (2011) Surface acetylation of cellulose nanocrystal and its reinforcing function in poly (lactic acid). Carbohyd Polym 83: 1834-1842. https://doi.org/10.1016/j.carbpol.2010.10.047

[33] Das S (2017) Mechanical and water swelling properties of waste paper reinforced unsaturated polyester composites. Constr Build Mater 138: 469-478. https://doi.org/10.1016/j.conbuildmat.2017.02.041

[34] Ashori A, Sheshmani S (2010) Hybrid composites made from recycled materials: Moisture absorption and thickness swelling behavior. Bioresour Technol 101: 4717-4720. https://doi.org/10.1016/j.biortech.2010.01.060

[35] Wirawan R, Sapuan SM, Yunus R, Abdan K (2012) Density and water absorption of sugarcane bagasse-filled poly (vinyl chloride) composites. Polym Polym Compos 20: 659-663. https://doi.org/10.1177/096739111202000710.

[36] Alamri H, Low IM (2012) Mechanical properties and water absorption behaviour of recycled cellulose fibre

reinforced epoxy composites. Polym Test 31: 620-628. https://doi.org/10.1016/j.polymertesting.2012.04.002

[37] Kamaludin NHI, Ismail H, Rusli A, Ting SS (2020) Thermal behavior and water absorption kinetics of polylactic acid/chitosan biocomposites. Iran Polym J 30 (2): 135-147. https://doi.org/10.1007/s13726-020-00879-5

[38] Reddy CR, Sardashti AP, Simon LC (2020) Preparation and characterization of polypropylene-wheat straw-clay composites. Compos Sci Technol 70 (12): 1674-1680. https://doi.org/ 10.1016/j.compscitech.2010.04.021

[39] Shi QF, Zhou CJ, Yue YY, Guo WH, Wu YQ, Wu QL (2012) Mechanical properties and in vitro degradation of electrospun bio-nanocomposites mats from PLA and cellulose nanocrystals. Carbohyd Polym 90: 301-308. https://doi.org/10.1016/j.carbpol.2012.05.042

Table captions

Table 1. Thermogravimetric analysis parameters of modified DPF/NCC/PLA composites.

Table 2. The thermal parameters of DSC of modified DPF/NCC/PLA composites.

Table 3. Diffusion coefficient, solubility, and permeability of modified DPF/NCC/PLA composites.

Figure captions

Figure 1. Schematic diagram of NCC and DPF/NCC/PLA modified composites preparation.

Figure 2. Flexural properties of modified DPF/NCC/PLA composites.

Figure 3. Tensile properties of modified DPF/NCC/PLA composites.

Figure 4. Impact properties of modified DPF/NCC/PLA composites.

Figure 5. Schematic diagram of KH570 modification mechanism.

Figure 6. FTIR spectra of interface modified NCC.

Figure 7. FTIR spectra of interface modified DPF.

Figure 8. TG curves of modified DPF/NCC/PLA composites.

Figure 9. DTG curves of modified DPF/NCC/PLA composites.

Figure 10. DSC curves of modified DPF/NCC/PLA composites.

Figure 11. Water absorption property of modified DPF/NCC/PLA composites: (a) within seven days; (b) within seven weeks.

Figure 12. Degradation properties of modified DPF/NCC/PLA composites.

Figure 13. SEM micrographs of modified DPF/NCC/PLA composites (×1000): (a) DPF/NCC/PLA, (b) KH570 DPF/NCC/PLA, (c) TMC201 DPF/NCC/PLA, (d) NaOH DPF/NCC/PLA, (e) PEG6000 DPF/NCC/PLA, (f) KH570/PEG6000 DPF/NCC/PLA

Table 1. Thermogravimetric analysis parameters of modified DPF/NCC/PLA composites.

Samples	T_{onset} /°C	T_{50} /°C	T_{max} /°C	R_{600} /%
DPF/NCC/PLA	291	345	346	4.6

KH570	291	344	351	5.4
TMC201	281	369	364	7.8
NaOH	256	322	328	4.6
PEG6000	276	334	337	7.8
KH570/PEG6000	279	338	340	8.8

Table 2. The thermal parameters of DSC of modified DPF/NCC/PLA composites.

Samples	T_g /°C	T_c/°C	ΔH_c /(J/g)	ΔH_m /(J/g)	T_{m1} /°C	T_{m2} /°C	χ_c /%
DPF/NCC/PLA	62.4	122.9	-19.78	17.18	151.5		22.4
KH570	62.6	112.0	-21.81	18.25	149		23.8
TMC201	62.0	110.6	-21.97	19.57	148.4	154.6	25.5
NaOH	61.4	113.3	-23.28	25.42	147.2	153.9	33.1
PEG6000	61.5	109.3	-22.01	19.11	148.1	154.6	24.9
KH570/PEG6000	61.9	109.7	-18.46	20.15	148.9	154.1	26.2

Table 3. Diffusion coefficient, solubility, and permeability of modified DPF/NCC/PLA composites.

Samples	$D\times10^{-13}(m^2/s)$	S(g/g)	$P\times10^{-14}(m^2/s)$
DPF/NCC/PLA	7.7164	0.0280	2.1606
KH570	7.1979	0.0228	1.6411
TMC201	6.6111	0.0230	1.5206
NaOH	6.1470	0.0224	1.3769
PEG6000	6.0231	0.0220	1.3251
KH570/PEG6000	5.9514	0.0215	1.2796

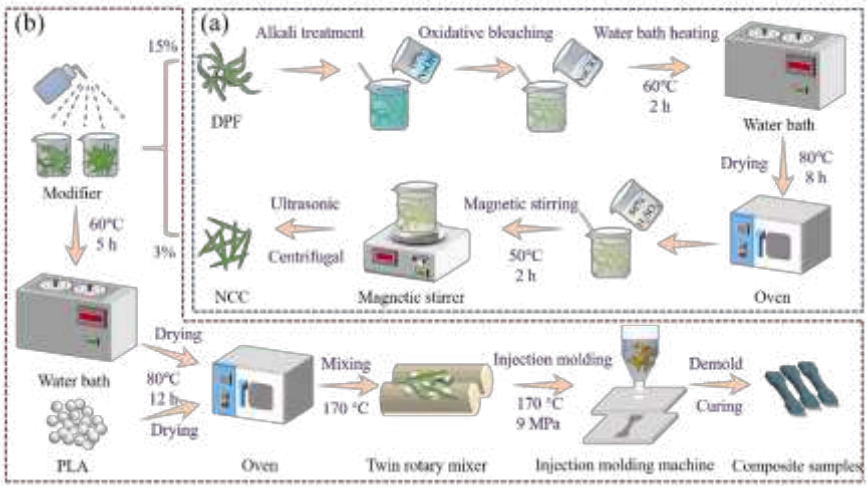

Figure 1. Schematic diagram of NCC and DPF/NCC/PLA modified composites preparation: (a) process of preparation of NCC; (b) process of preparation of DPF/NCC/PLA modified composites.

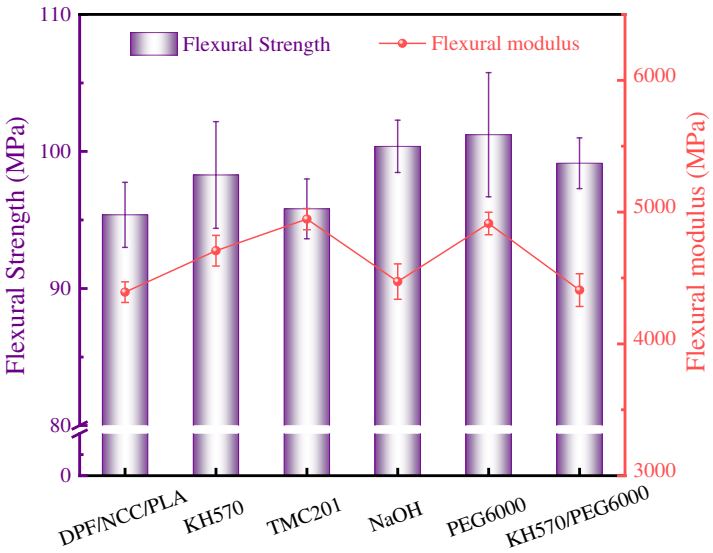

Figure 2. Flexural properties of modified DPF/NCC/PLA composites.

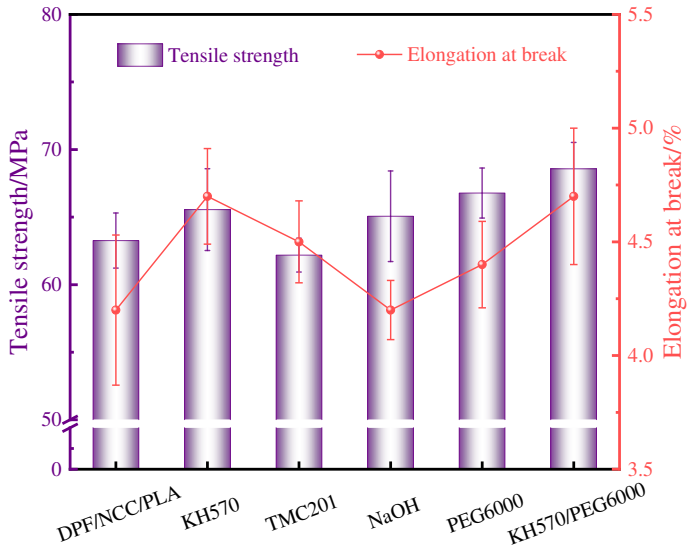

Figure 3. Tensile properties of modified DPF/NCC/PLA composites.

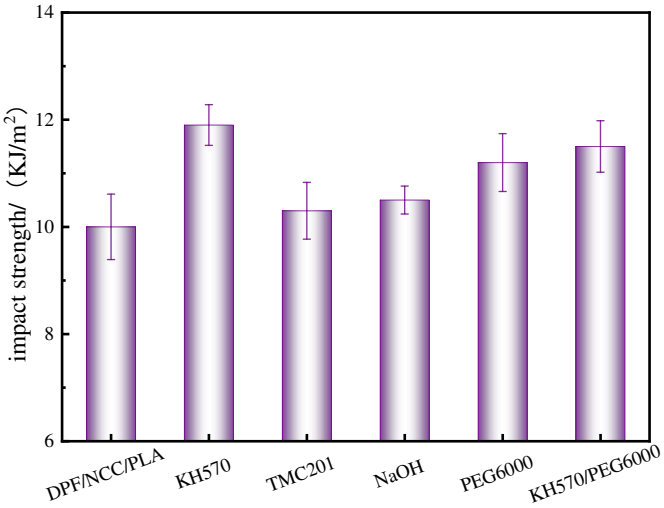

Figure 4. Impact properties of modified DPF/NCC/PLA composites.

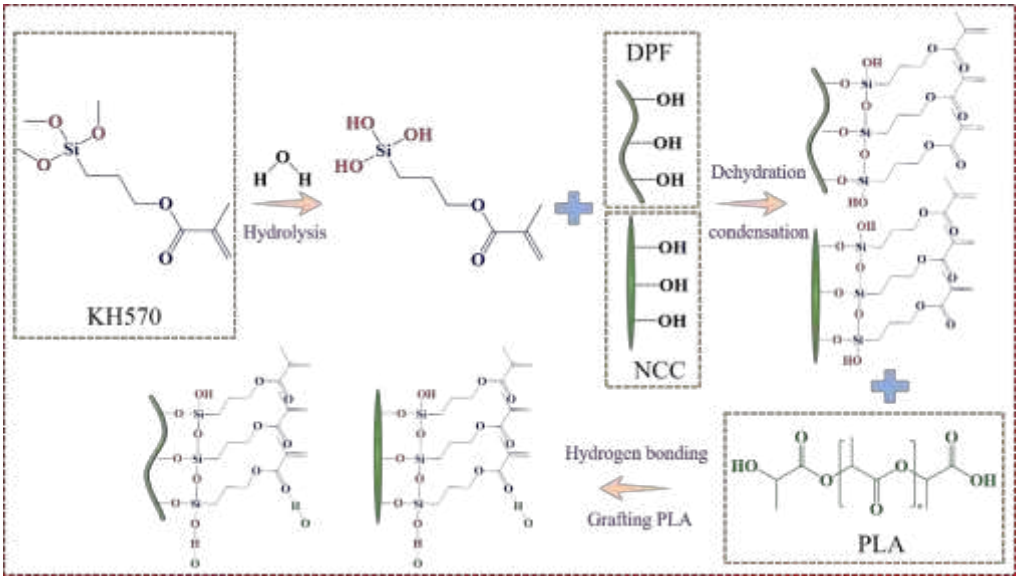

(a)

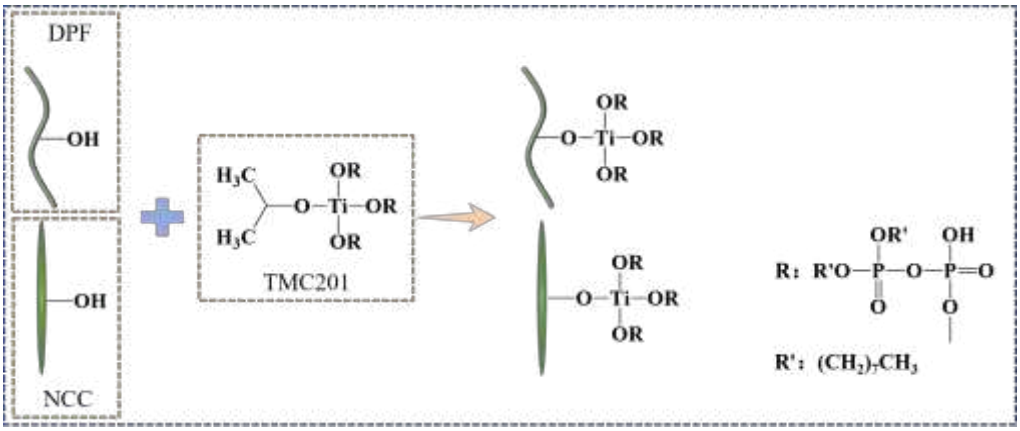

(b)

Figure 5. Schematic diagram of modification mechanism: (a) KH570; (b) TMC201.

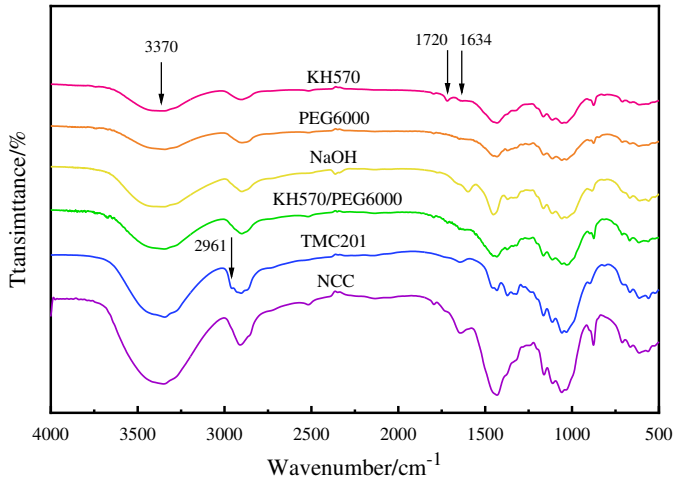

Figure 6. FTIR spectra of interface modified NCC.

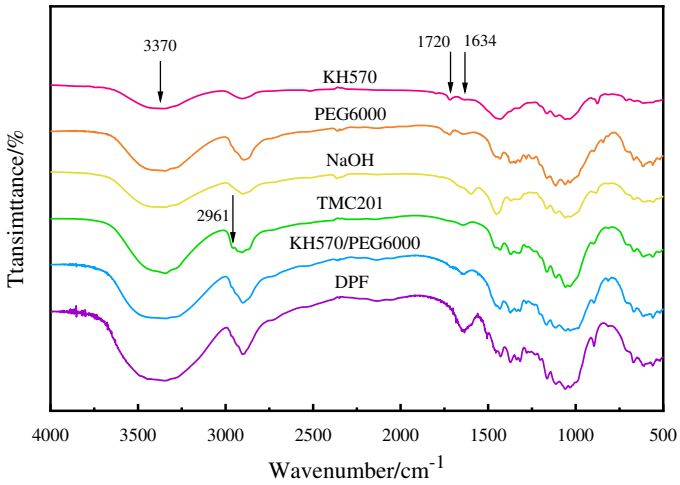

Figure 7. FTIR spectra of interface modified DPF.

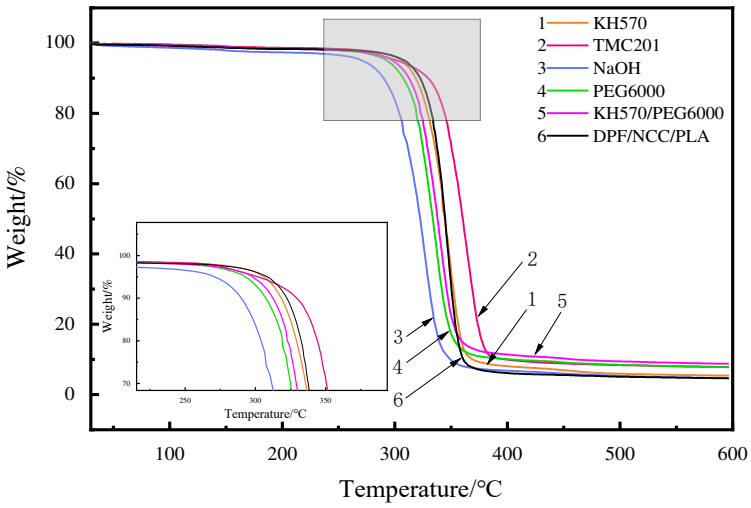

Figure 8. TG curves of modified DPF/NCC/PLA composites.

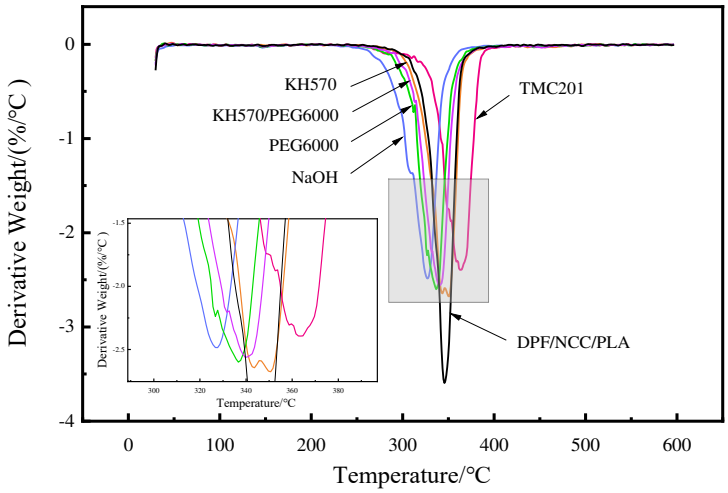

Figure 9. DTG curves of modified DPF/NCC/PLA composites.

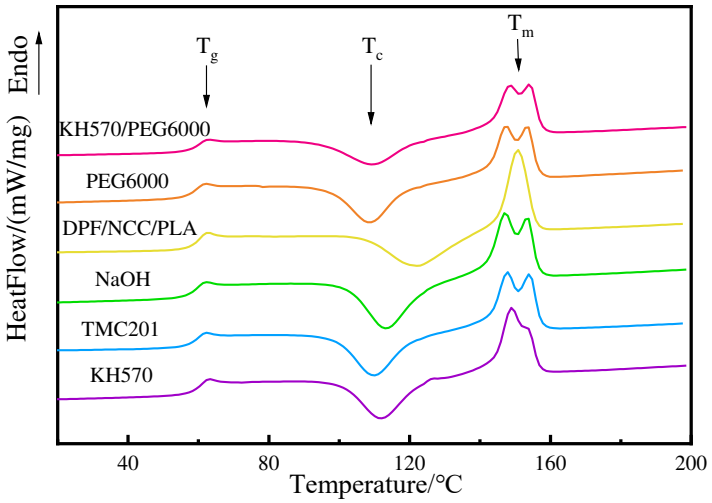

Figure 10. DSC curves of modified DPF/NCC/PLA composites.

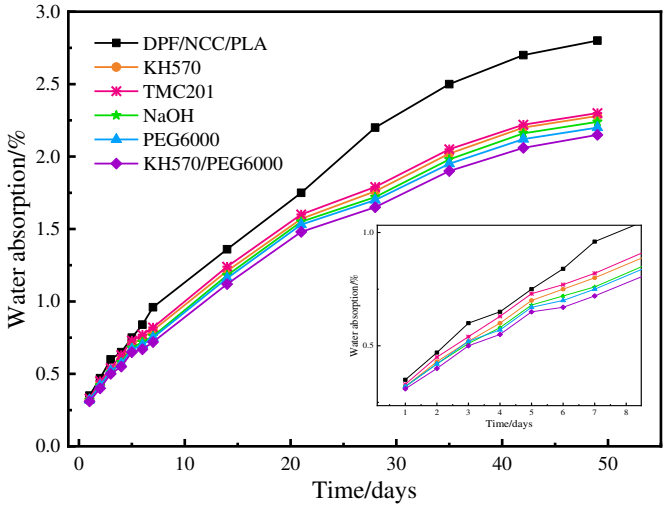

Figure 11. Water absorption property of modified DPF/NCC/PLA composites.

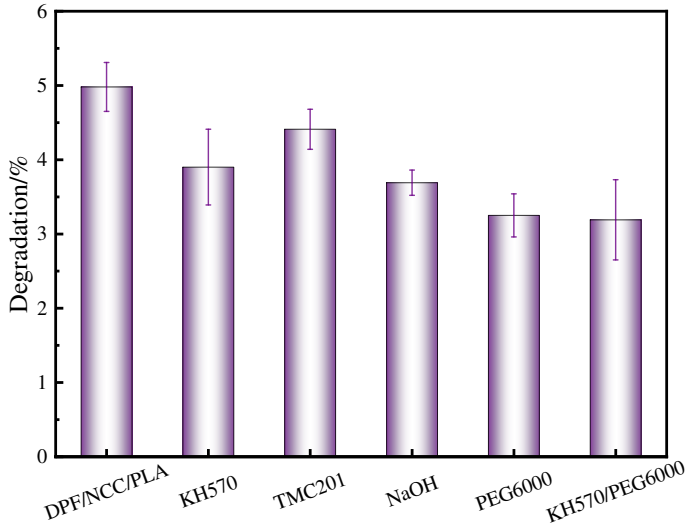

Figure 12. Degradation properties of modified DPF/NCC/PLA composites.

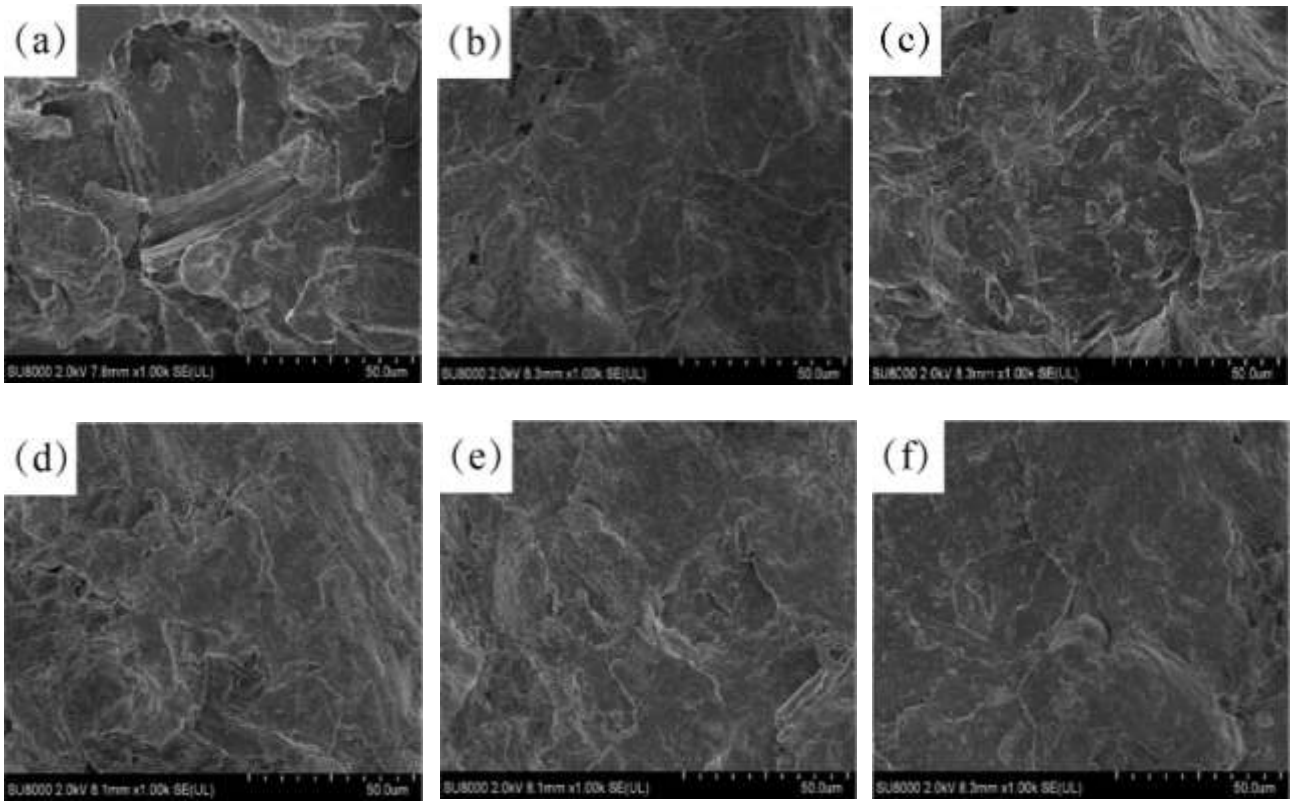

Figure 13. SEM micrographs of modified DPF/NCC/PLA composites (×1000): (a) DPF/NCC/PLA, (b) KH570 DPF/NCC/PLA, (c) TMC201 DPF/NCC/PLA, (d) NaOH DPF/NCC/PLA, (e) PEG6000 DPF/NCC/PLA, (f) KH570/PEG6000 DPF/NCC/PLA

Figures

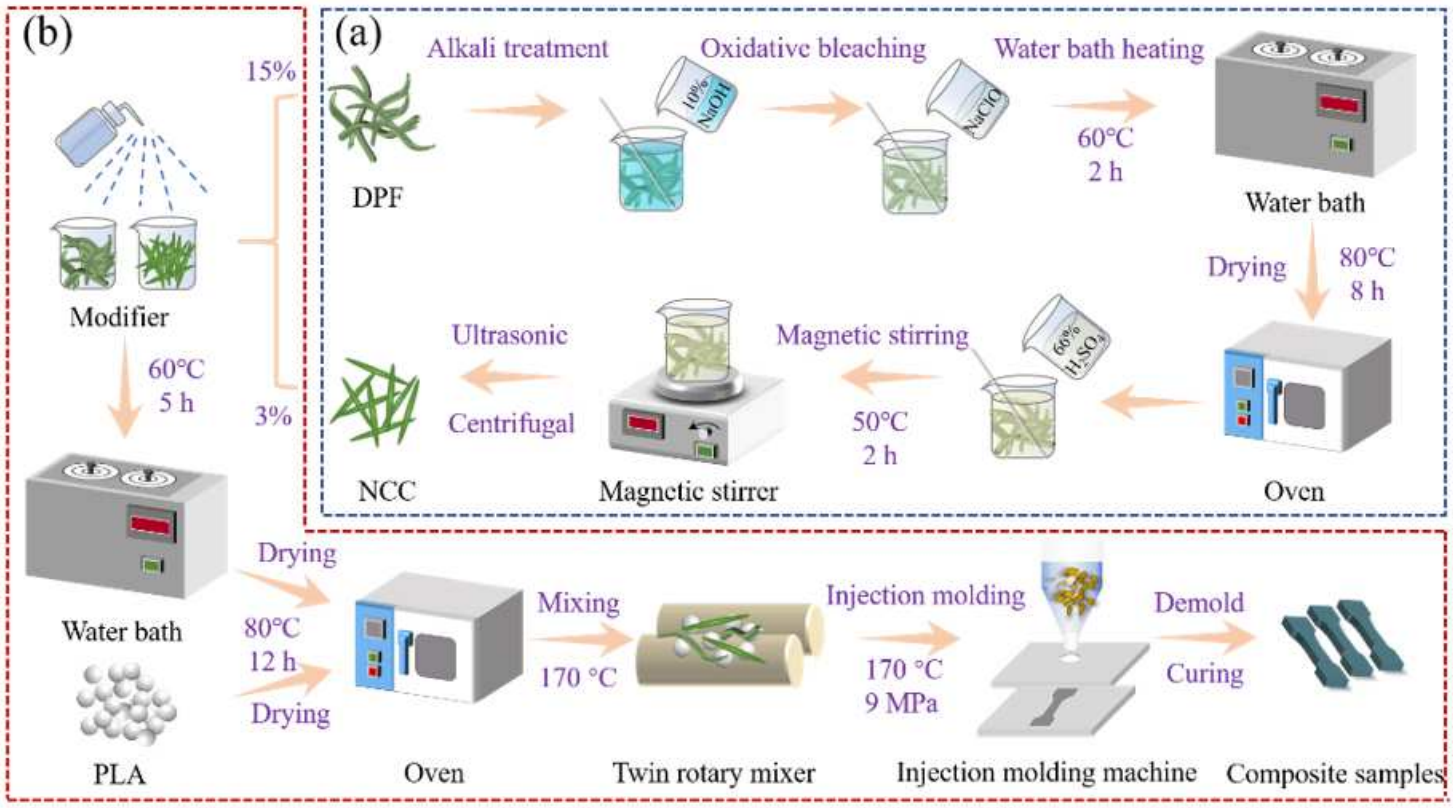

Figure 1

Schematic diagram of NCC and DPF/NCC/PLA modified composites preparation: (a) process of preparation of NCC, (b) process of preparation of DPF/NCC/PLA modified composites.

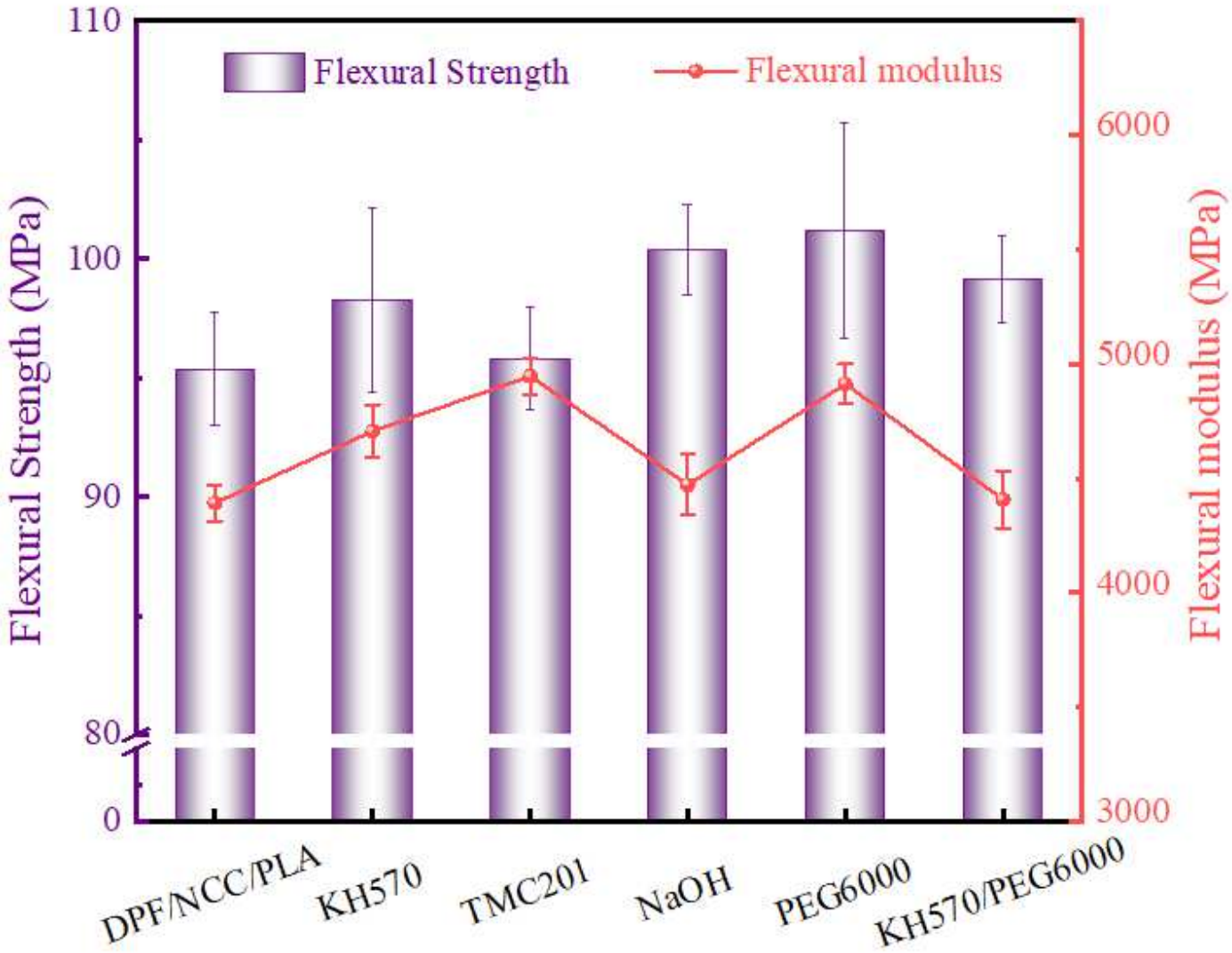

Figure 2

Flexural properties of modified DPF/NCC/PLA composites.

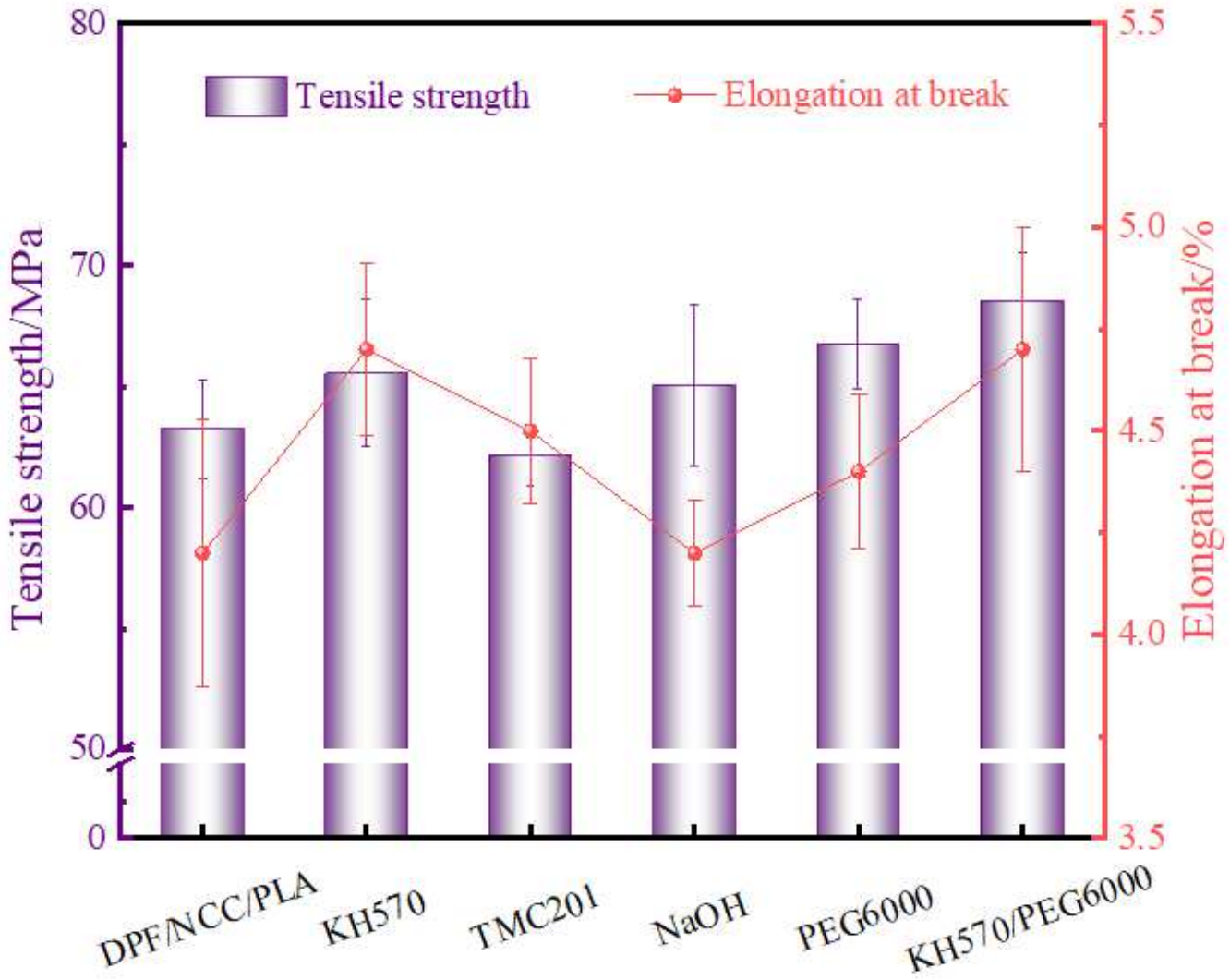

Figure 3

Tensile properties of modified DPF/NCC/PLA composites.

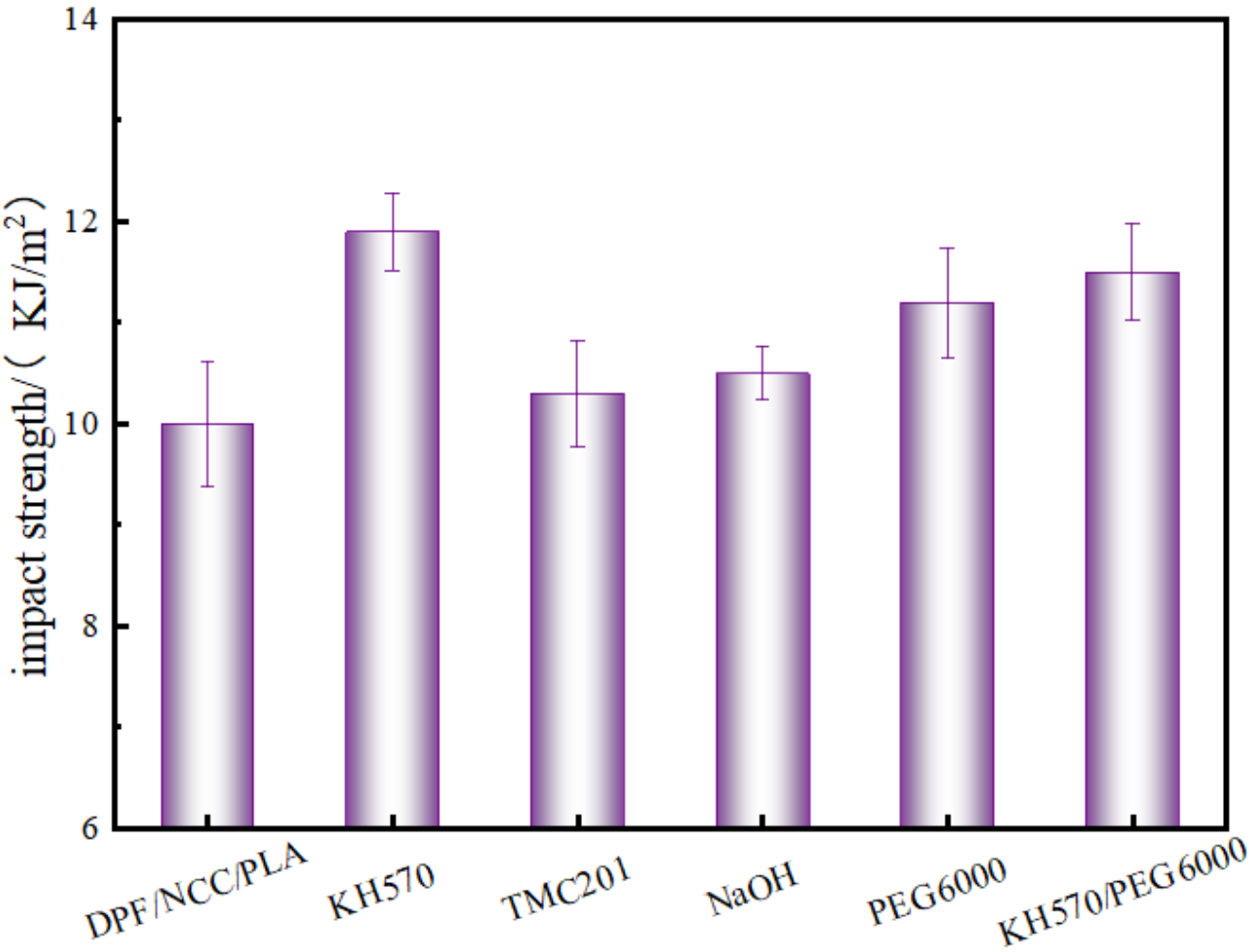

Figure 4

Impact properties of modified DPF/NCC/PLA composites.

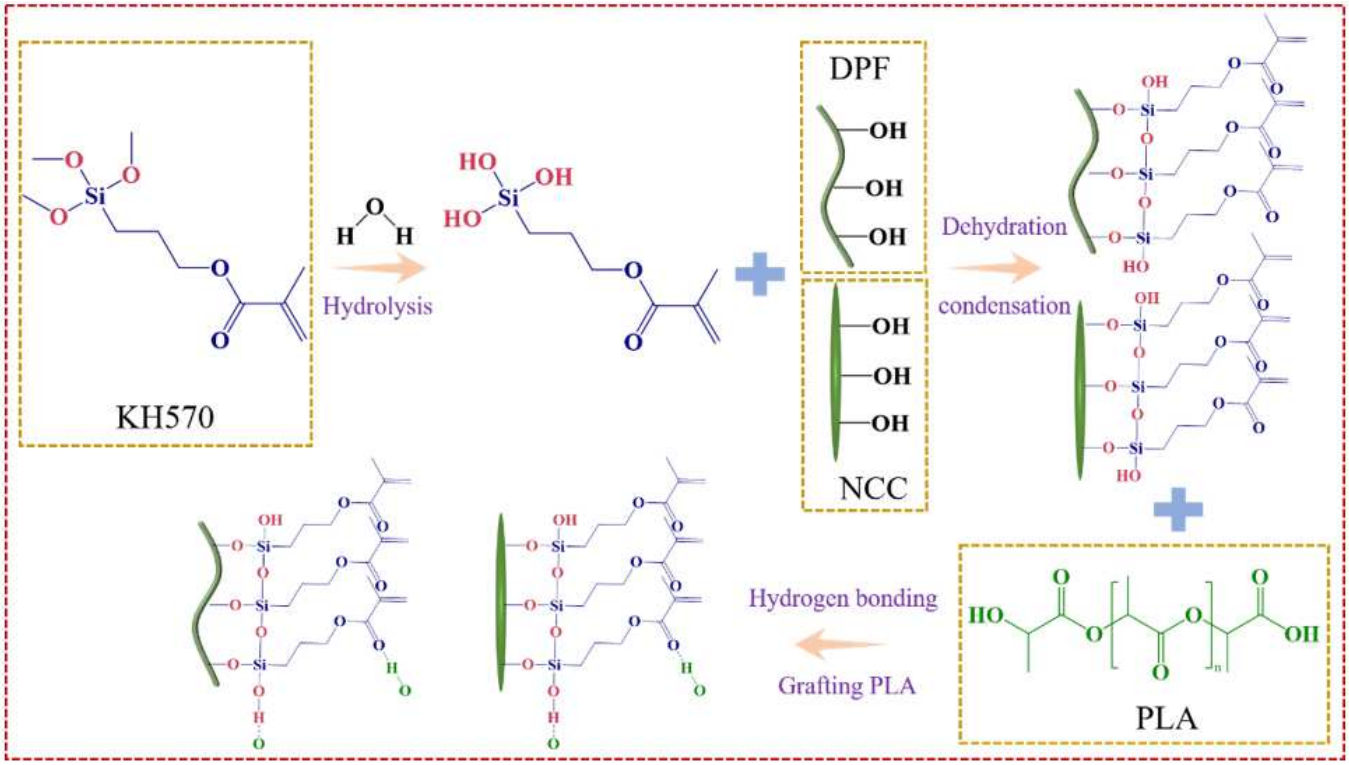

(a)

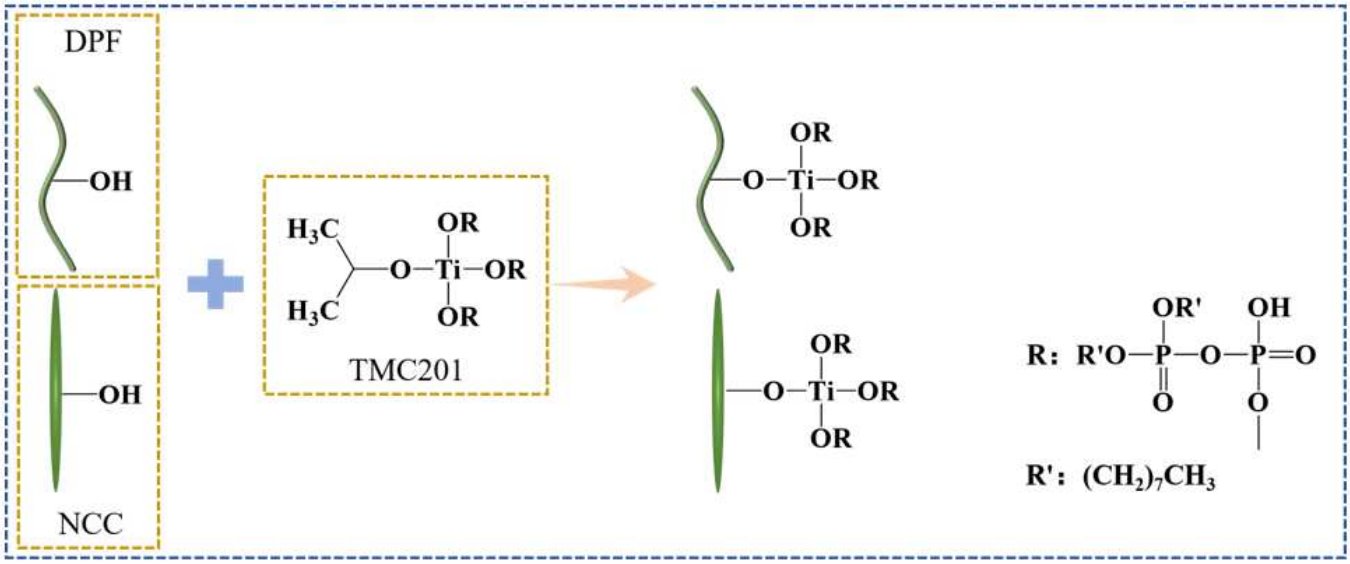

(b)

Figure 5

Schematic diagram of modification mechanism: (a) KH570, (b) TMC201.

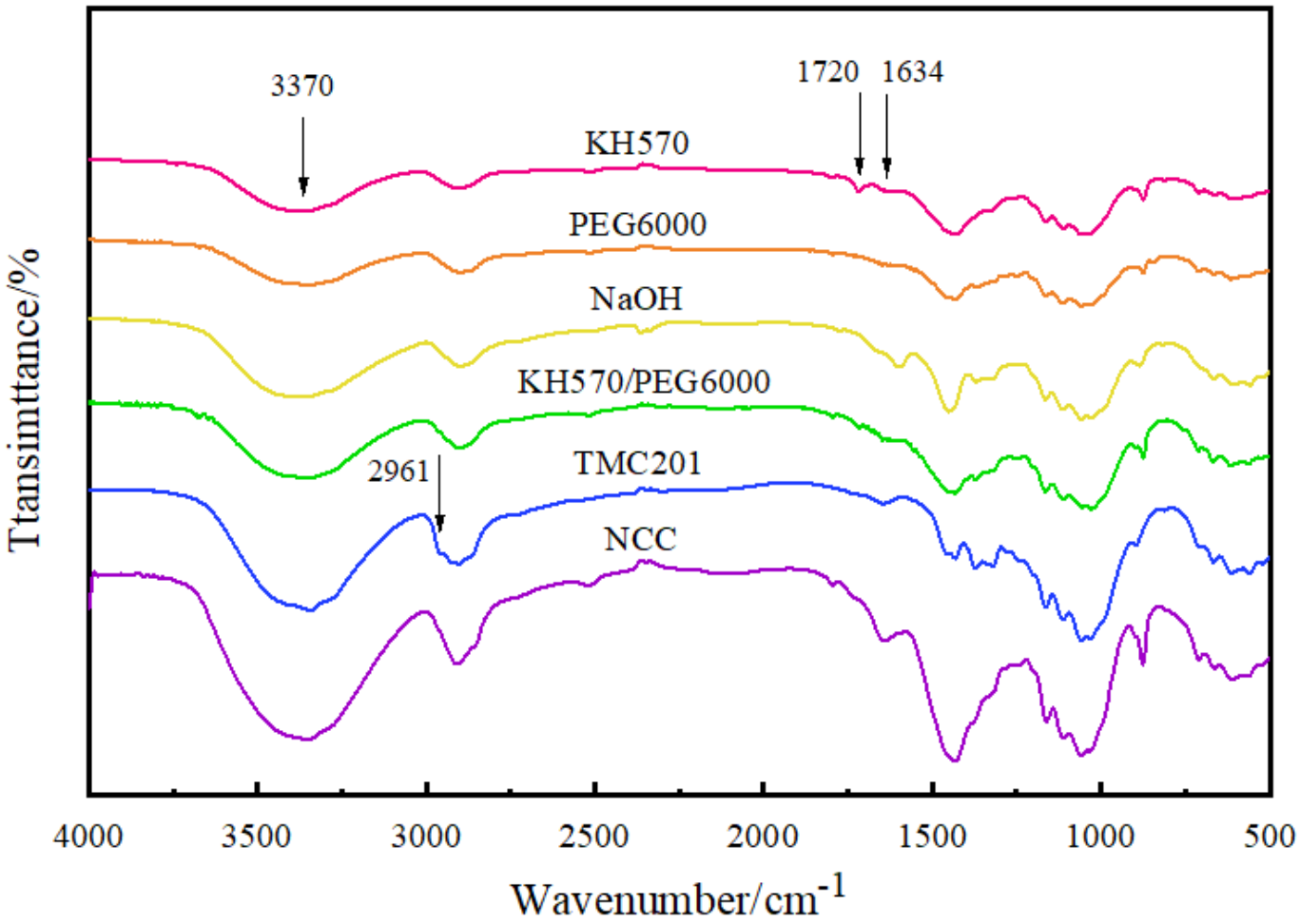

Figure 6

FTIR spectra of interface modified NCC.

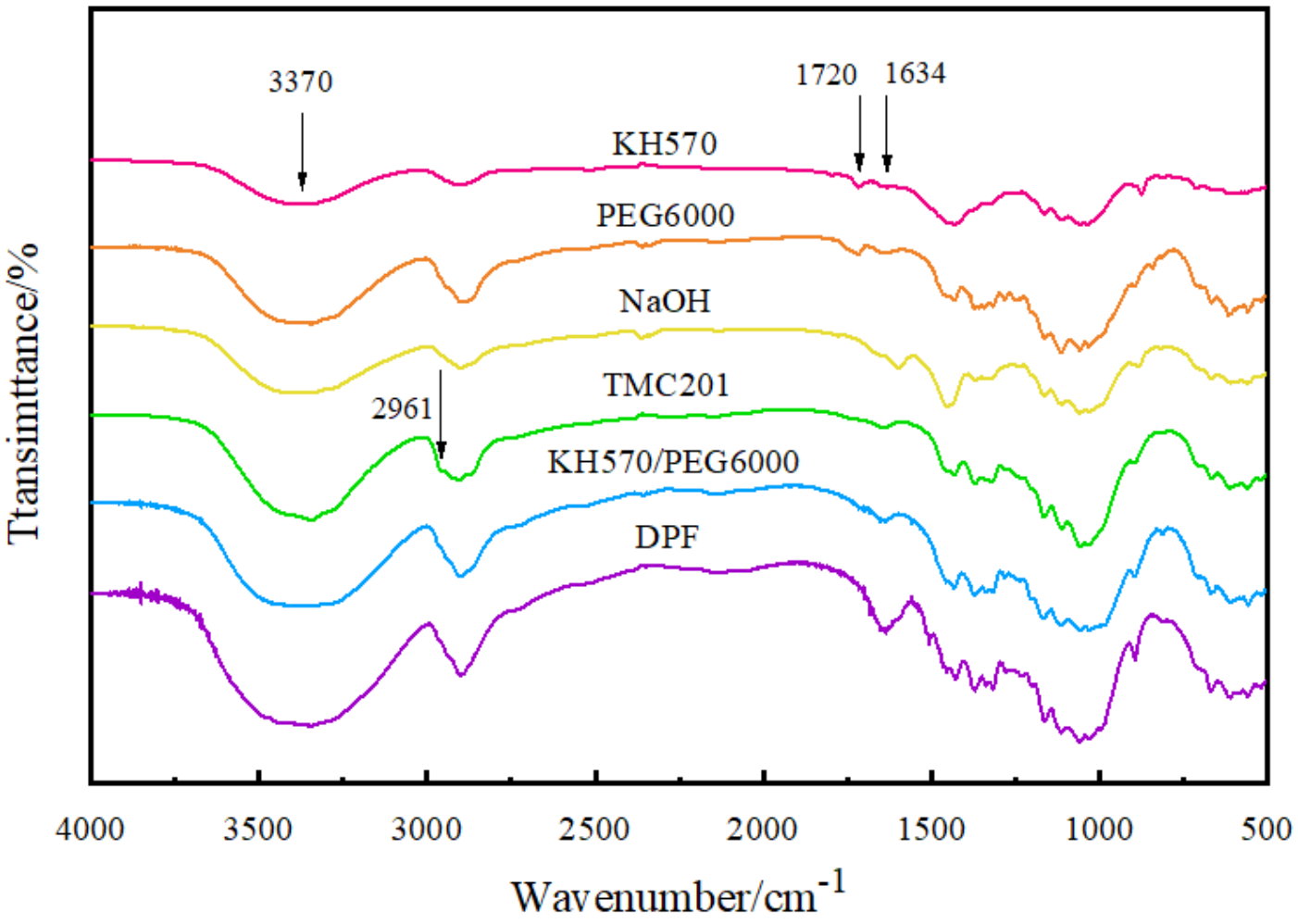

Figure 7

FTIR spectra of interface modified DPF.

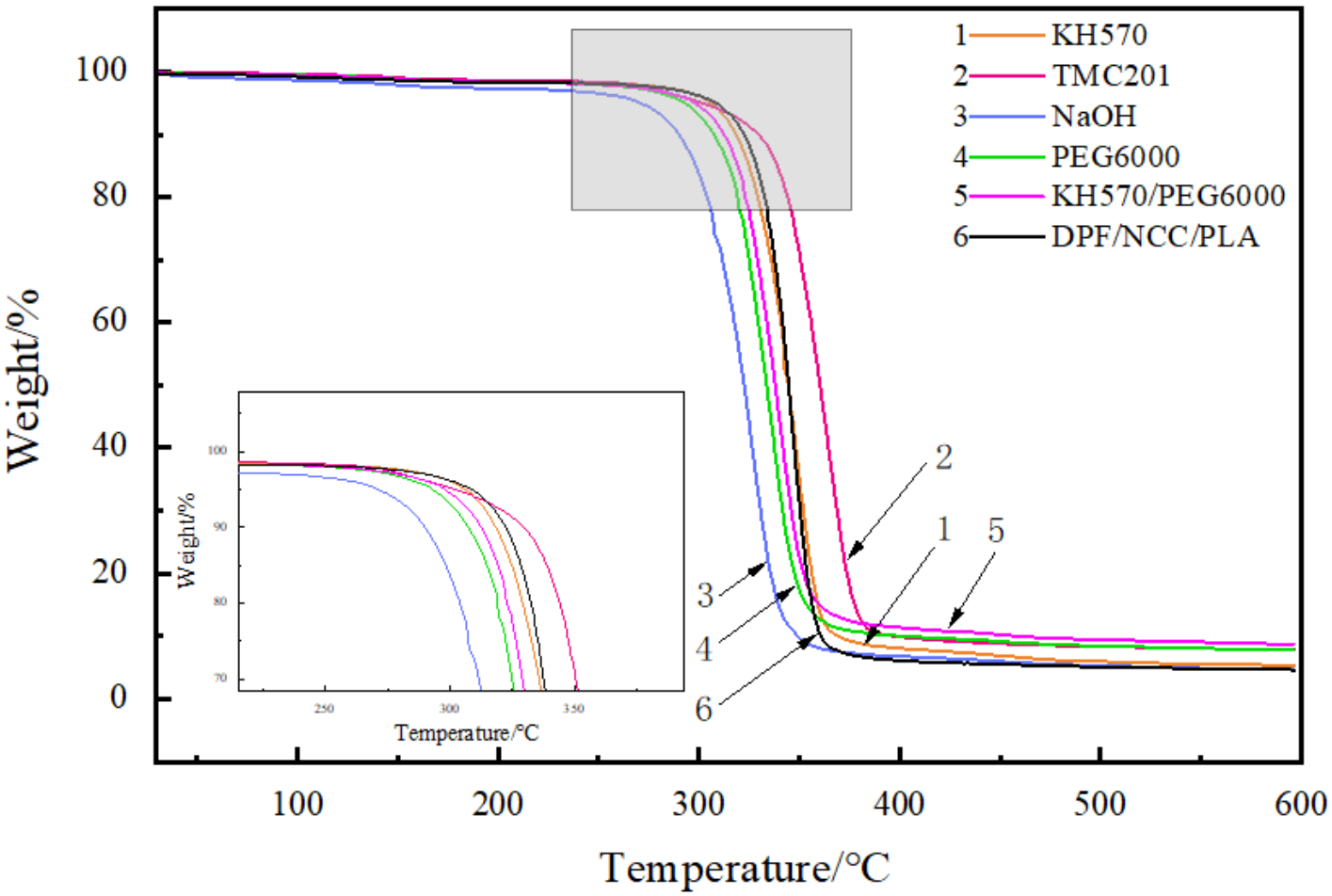

Figure 8

TG curves of modified DPF/NCC/PLA composites.

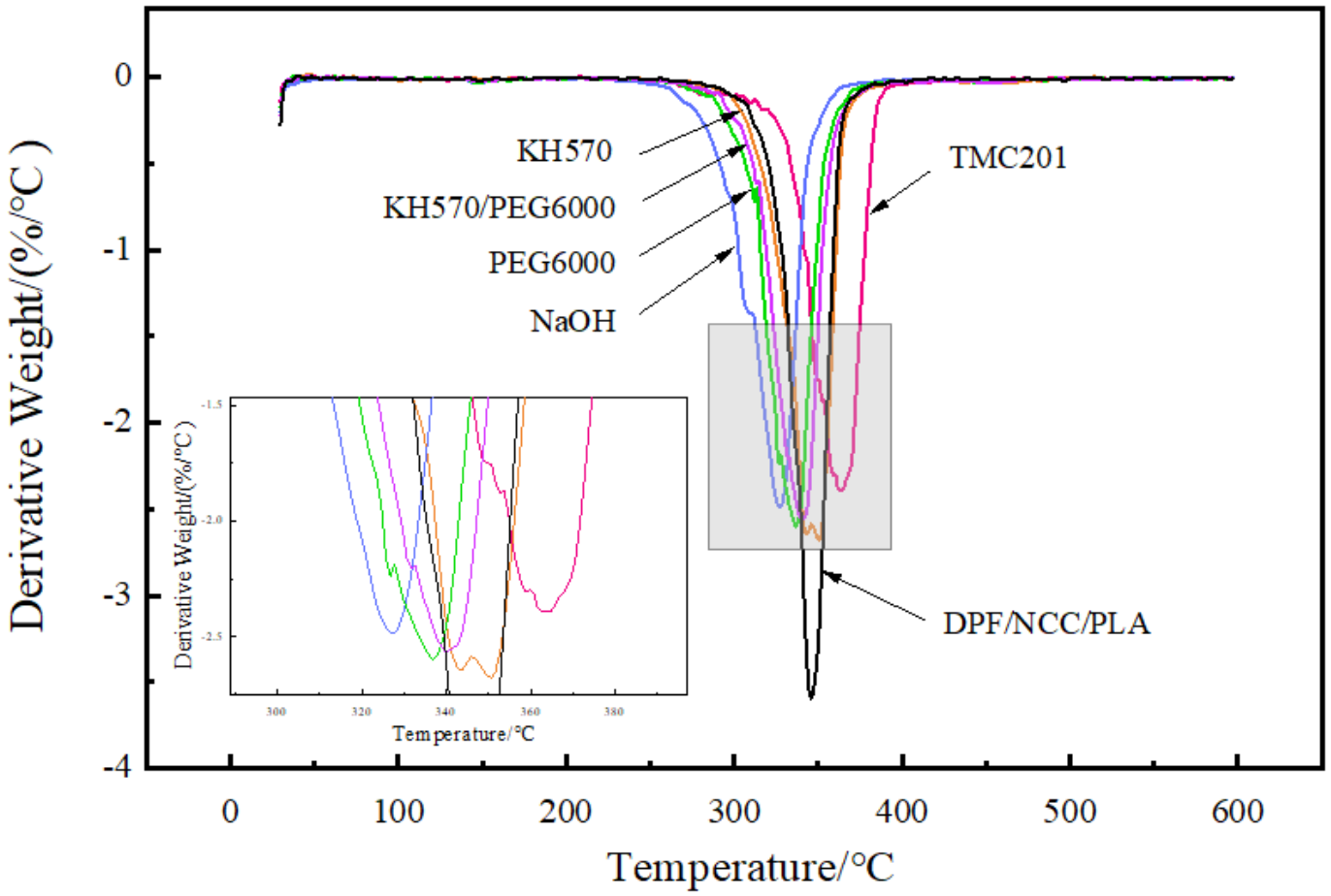

Figure 9

DTG curves of modified DPF/NCC/PLA composites.

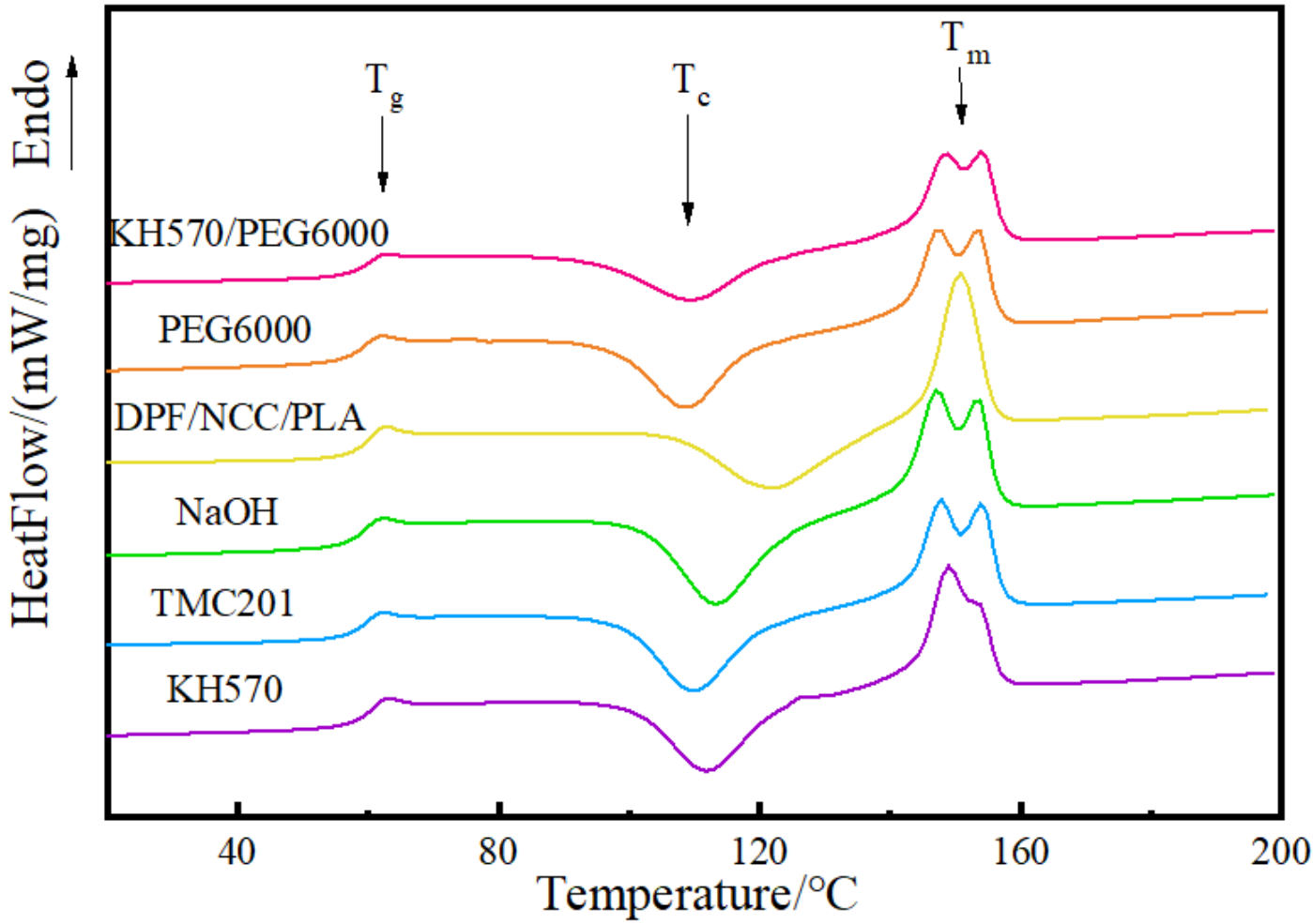

Figure 10

DSC curves of modified DPF/NCC/PLA composites.

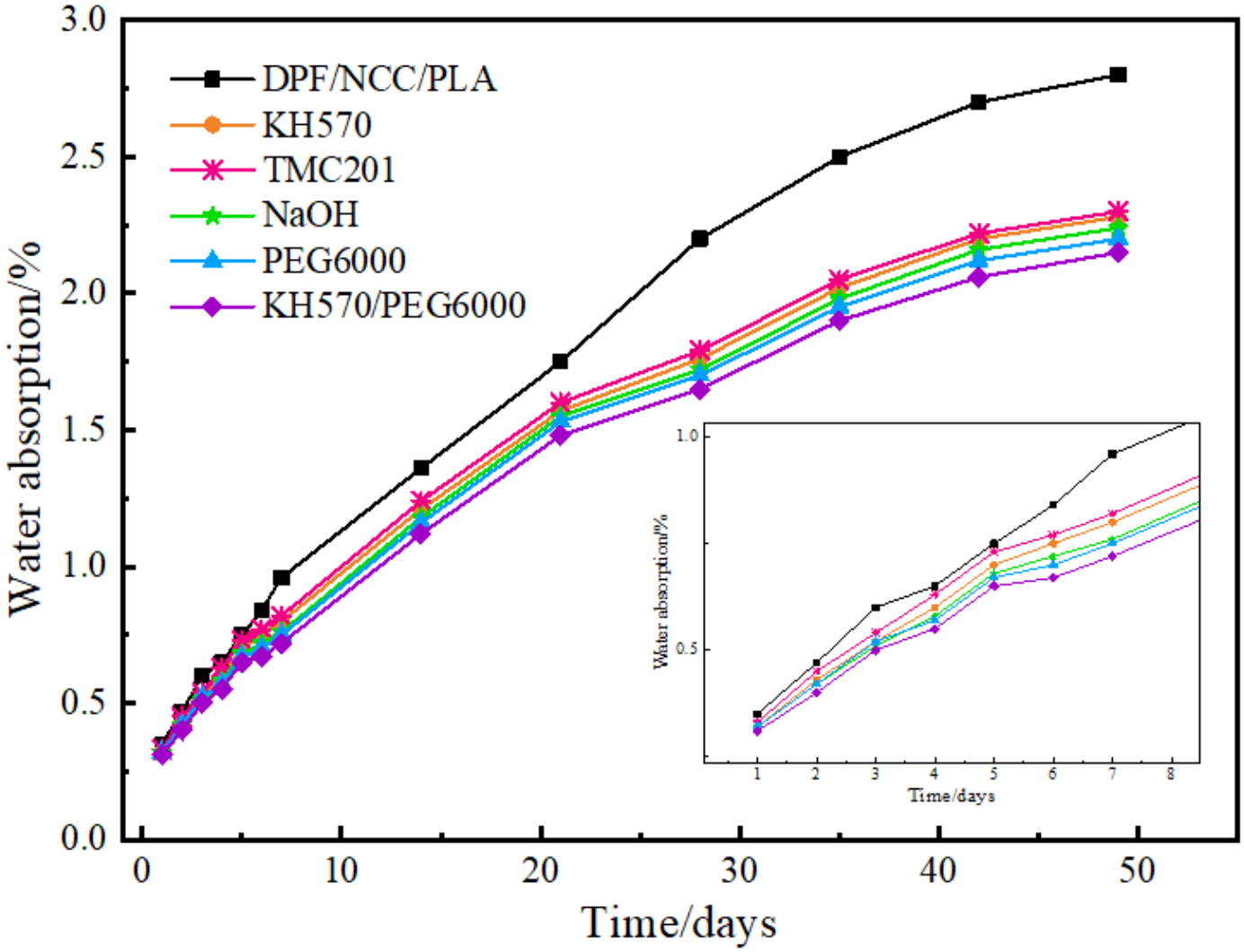

Figure 11

Water absorption property of modified DPF/NCC/PLA composites.

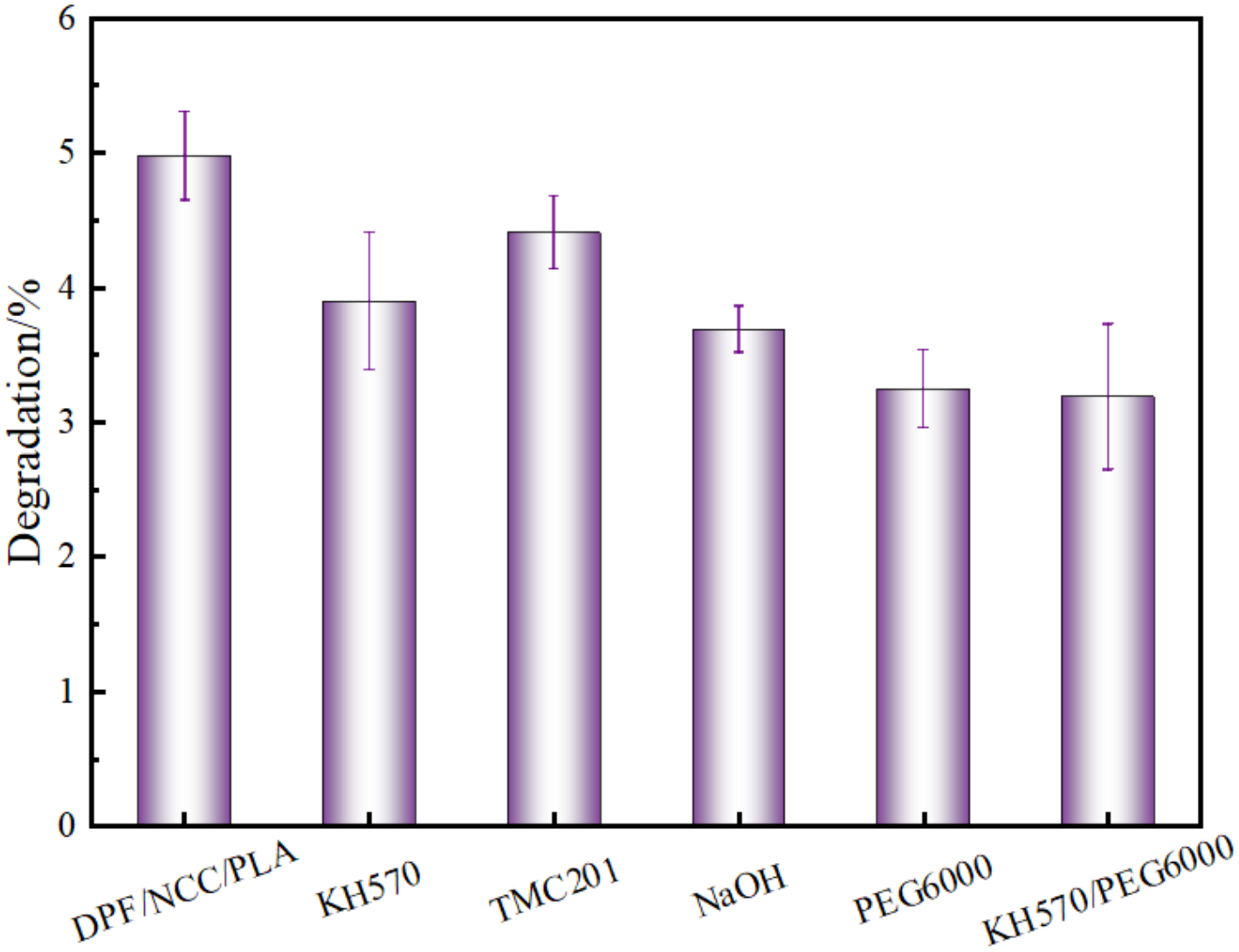

Figure 12

Degradation properties of modified DPF/NCC/PLA composites.

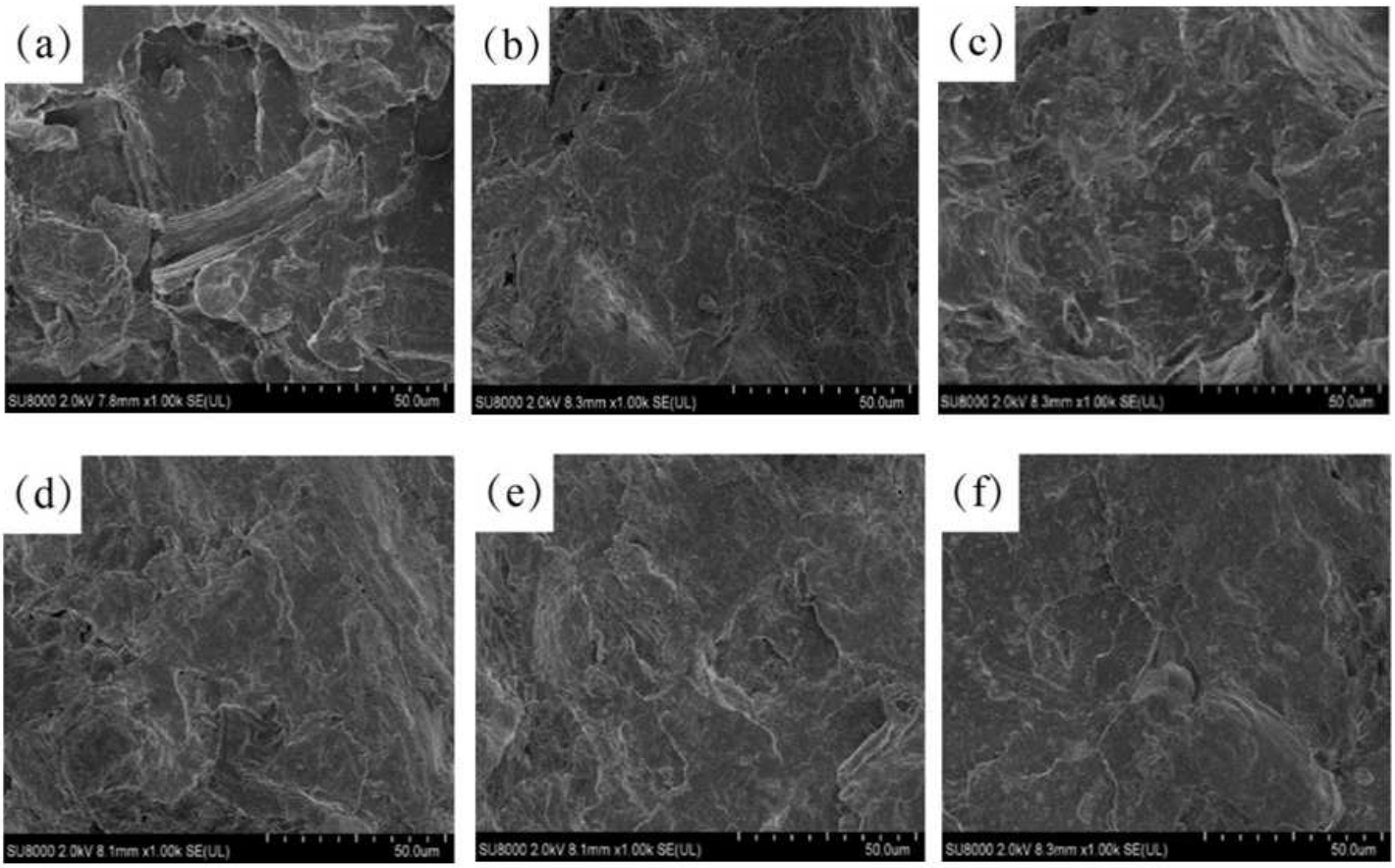

Figure 13

SEM micrographs of modified DPF/NCC/PLA composites (×1000): (a) DPF/NCC/PLA, (b) KH570 DPF/NCC/PLA, (c) TMC201 DPF/NCC/PLA, (d) NaOH DPF/NCC/PLA, (e) PEG6000 DPF/NCC/PLA, (f) KH570/PEG6000 DPF/NCC/PLA